Quantifying critical N dilution curves across G × E × M effects for potato using a partially-pooled Bayesian hierarchical method

--Manuscript Draft--

Manuscript Number:	
Article Type:	Research paper
Section/Category:	Crop Management
Keywords:	critical N concentration; critical nitrogen dilution curve; nitrogen nutrition index; nitrogen use efficiency; potato; Bayesian; genotype-by-environment-by-management interactions
Corresponding Author:	Brian Joseph Bohman, Ph.D. University of Minnesota Twin Cities: University of Minnesota Twin Cities UNITED STATES
First Author:	Brian Joseph Bohman, Ph.D.
Order of Authors:	Brian Joseph Bohman, Ph.D.
	Michael J. Culshaw-Maurer
	Feriel Ben Abdallah
	Claudia Giletto
	Gilles Bélanger
	Fabián G. Fernández
	Yuxin Miao
	David J. Mulla
	Carl J. Rosen
Abstract:	Multiple critical N dilution curves [CNDCs] have been previously developed for potato; however, attempts to directly compare differences in CNDCs across genotype [G], environment [E], and management [M] interactions have been confounded by non-uniform statistical methods, biased experimental data, and lack of proper quantification of uncertainty in the critical N concentration [$\%N_c$]. This study implements a partially-pooled Bayesian hierarchical method to develop CNDCs for previously published and newly reported experimental data, systematically evaluates the difference in $\%N_c$ [$\Delta\%N_c$] across G × E × M effects, and directly compare CNDCs from the Bayesian framework to CNDCs from conventional statistical methods. The partially-pooled Bayesian hierarchical method implemented in this study has the advantage of being less susceptible to inferential bias at the level of individual G × E × M interactions compared to alternative statistical methods that result from insufficient quantity and quality of experimental datasets (e.g., unbalanced distribution of N limiting and non-N limiting observations). This method also allows for a direct statistical comparison of differences in $\%N_c$ across levels of the G × E × M interactions. Where found to be significant, $\Delta\%N_c$ was attributed to variation in the timing of tuber initiation (e.g., maturity class) and the relative rate of tuber bulking (e.g., planting density) across G x E × M interactions. In addition to using the median value for $\%N_c$ (i.e., CNDC), the lower and upper boundary values for the credible region (i.e., $CNDC_{lo}$ and $CNDC_{up}$) derived using the Bayesian framework should be used in calculation of N nutrition index (and other calculations) to account for uncertainty in $\%N_c$. Overall, this study provides additional evidence that $\%N_c$ is dependent upon G × E × M interactions; therefore, evaluation of crop N status or N use efficiency must account for variation in $\%N_c$ across G × E × M interactions.
Suggested Reviewers:	Ignacio Ciampitti ciampitti@ksu.edu Dr. Ciampitti has authored a number of studies on similar topics to this manuscript and would be an excellent reviewer/editor.

	Gilles Lemaire gilles.lemaire.inra@gmail.com Dr. Lemaire has authored a number of studies on similar topics to this manuscript and would be an excellent reviewer.
	David Makowski makowski@grignon.inra.fr Dr. Makowski has authored a number of studies on similar topics to this manuscript and would be an excellent reviewer.
	Javier Fernández jafernandez@ksu.edu Dr. Fernández has authored a number of studies on similar topics to this manuscript and would be an excellent reviewer.
	Victor Sadras victor.sadras@sa.gov.au Dr. Sadras has authored a number of studies on similar topics to this manuscript and would be an excellent reviewer.

- Critical N dilution curves [CNDCs] for potato are subject to G x E x M effects
- Bayesian methods can quantify uncertainty in critical N concentration [$\%N_c$]
- Partial pooling Bayesian method enables direct comparison of G x E x M effects
- Variation in $\%N_c$ for potato due to tuber initiation timing and tuber bulking rate
- N use efficiency and N nutrition index depend on $\%N_c$ variability and uncertainty

1 **Quantifying critical N dilution curves across G × E × M effects for potato using a partially-**

2 **pooled Bayesian hierarchical method**

3 Brian J. Bohman[1*], Michael J. Culshaw-Maurer[2], Feriel Ben Abdallah[3], Claudia Giletto[4], Gilles

4 Bélanger[5], Fabián G. Fernández[1], Yuxin Miao[1], David J. Mulla[1], and Carl J. Rosen[1]

5   1. Department of Soil, Water, and Climate, University of Minnesota. 1991 Upper Buford

6   Circle, St. Paul MN 55108

7   2. CyVerse, University of Arizona, Tuscon, AZ

8   3. Productions in Agriculture Department, Crop Production Unit, Walloon Agricultural

9   Research Centre (CRA-W), Gembloux, Belgium

10   4. Unidad Integrada Balcarce, Facultad de Ciencias Agrarias (UNMdP)-INTA Balcarce. Ruta

11   226 km 73,5 (7620) Balcarce, Buenos Aires, Argentina

12   5. Science and Technology Branch, Agriculture and Agri-Food Canada, Québec City, Canada

13 * Corresponding Author: bohm0072@umn.edu

14

15 **Abstract**: Multiple critical N dilution curves [CNDCs] have been previously developed for potato;

16 however, attempts to directly compare differences in CNDCs across genotype [G], environment

17 [E], and management [M] interactions have been confounded by non-uniform statistical methods,

18 biased experimental data, and lack of proper quantification of uncertainty in the critical N

19 concentration [$\%N_c$]. This study implements a partially-pooled Bayesian hierarchical method to

20 develop CNDCs for previously published and newly reported experimental data, systematically

21 evaluates the difference in $\%N_c$ [$\Delta\%N_c$] across $G \times E \times M$ effects, and directly compare CNDCs

22 from the Bayesian framework to CNDCs from conventional statistical methods. The partially-

23 pooled Bayesian hierarchical method implemented in this study has the advantage of being less

24 susceptible to inferential bias at the level of individual $G \times E \times M$ interactions compared to

25 alternative statistical methods that result from insufficient quantity and quality of experimental

26 datasets (e.g., unbalanced distribution of N limiting and non-N limiting observations). This method

27 also allows for a direct statistical comparison of differences in $\%N_c$ across levels of the $G \times E \times$

28 M interactions. Where found to be significant, $\Delta\%N_c$ was attributed to variation in the timing of

29 tuber initiation (e.g., maturity class) and the relative rate of tuber bulking (e.g., planting density)

30 across $G \times E \times M$ interactions. In addition to using the median value for $\%N_c$ (i.e., CNDC), the

31 lower and upper boundary values for the credible region (i.e., $CNDC_{lo}$ and $CNDC_{up}$) derived using

32 the Bayesian framework should be used in calculation of N nutrition index (and other calculations)

33 to account for uncertainty in $\%N_c$. Overall, this study provides additional evidence that $\%N_c$ is

34 dependent upon $G \times E \times M$ interactions; therefore, evaluation of crop N status or N use efficiency

35 must account for variation in $\%N_c$ across $G \times E \times M$ interactions.

1. Introduction

53 Identifying optimal crop nitrogen [N] status to maximize growth and yield production is an elusive

54 goal. Traditionally, either the yield-goal approach or rate-response curves have been used to

55 identify optimal N fertilizer application rate (Morris et al., 2018). The N nutrition index [NNI] is

56 an alternative approach to the current paradigm and comprises a well-developed framework to

57 determine optimal crop N status (Lemaire et al., 2019). Typically, NNI is used to determine crop

58 N status using whole plant analysis and to direct adaptive N management within a growing season

59 (Houlès et al., 2007; Morier et al., 2015). Unlike the yield-goal or rate-response approach where

60 the optimal N fertilizer rate is empirically based on the marginal economic returns to yield from N

61 fertilizer (i.e., economic optimum N rate [EONR]) under a given set of genotype [G], environment

62 [E], and management [M] factors (Morris et al., 2018; Nigon et al., 2019), the NNI framework has

63 conventionally been considered generalizable across $E \times M$ effects (e.g., year-to-year, geographic,

64 or cultural practices variability) and can be defined for any particular G effect (e.g., crop species

65 or cultivar). In this manner, NNI is considered to represent intrinsic physiological properties

66 (Sadras & Lemaire, 2014) rather than a parameter otherwise subject to variation under

67 environmental conditions (e.g., net soil N supply) or management practices (e.g., rate, source,

68 timing, and placement of N fertilizer).

69 The NNI approach is defined based on the allometric relationship of declining plant N

70 concentration [$\%N_{Plant}$] with increasing plant biomass, referred to as the critical N dilution curve

71 [CNDC], which defines the critical N concentration [$\%N_c$] below which relative growth rate is

72 reduced (Gastal et al., 2015):

73 $\%N_c = a\ W^{-b}$ [1]

74   where W represents dry weight plant biomass, and a and b are empirically fitted parameters.

75   Parameter a is numerically equivalent to %N_c expressed in units of g N 100 g^{-1} when W is equal

76   to 1 Mg ha^{-1}, and parameter b effectively represents the rate of decline in %N_c as W increases.

77   Using the CNDC, NNI values are then calculated as ratio of %N_{Plant} and %N_c:

78   $$NNI = \%N_{Plant} / \%N_c \qquad [2]$$

79   When NNI is greater than 1.0, crop N status is said to be in excess, and crop growth is not limited

80   by N, while when NNI is less than 1.0, crop N status is deficient, and crop growth is limited by N.

81   At NNI equal to 1.0, crop N status is optimal (Lemaire & Gastal, 1997).

82   A robust theoretical framework has been developed to explain decline in N concentration as

83   biomass increases, but the application of this theory is most commonly restricted to the vegetative

84   period where only metabolic and structural tissues are present (Greenwood et al., 1990; Justes et

85   al., 1994; Sadras & Lemaire, 2014). Dilution of N in vegetative tissue occurs in relationship to an

86   increasing proportion of structural biomass, with low N concentration, relative to metabolic (i.e.,

87   photosynthetic) biomass, with high N concentration (Lemaire & Gastal, 1997; Gastal et al., 2015).

88   Multiple previous studies have extended and empirically validated the CNDC relationships beyond

89   its typical applications to describe declining N concentration over the entire crop growth cycle,

90   including periods of reproductive growth, by including consideration of storage tissues in addition

91   to structural and metabolic tissues (Greenwood et al., 1986; Duchenne et al., 1997; Plénet &

92   Lemaire, 2000; Herrmann & Taube, 2004). Dilution of N beyond the vegetative period primarily

93   occurs as low N biomass (i.e., starch) accumulates in storage tissues such as grain or tubers, and

94   the rate of decline is determined by the relative N concentration in storage biomass compared to

95   vegetative biomass (Duchenne et al., 1997; Plénet & Lemaire, 2000). Duchenne et al. (1997)

96 observed that as an increasing proportion of biomass accumulates in tubers, the rate of decline in

97 N concentration increases with increasing biomass. Certain crops, such as potato, exclusively use

98 a CNDC based on whole plant biomass due to the complex relationship between vine growth and

99 tuber production (Duchenne et al., 1997; Bélanger et al., 2001a; Giletto & Echeverría, 2015; Ben

100 Abdallah et al., 2016). Despite the validity of this approach, interpretating variation in CNDC

101 observed between cultivars and geographies has been challenging.

102 However, recent work by Giletto et al. (2020) identified a mechanistic relationship underpinning

103 the observed empirical relationships in N dilution for potato. The CNDC based on whole plant

104 biomass reflects dilution in both the tuber and vine biomass, individually, and the increasing

105 proportion of biomass allocated to low concentrations of N in biomass (i.e., tubers) as whole plant

106 biomass increases. Giletto et al. (2020) also observed that varieties and locations with a greater

107 proportion of biomass allocated to tubers have a greater value for parameter *b* of the CNDC, where

108 parameter *b* of the CNDC represents the relative rate of decline in $\%N_c$ as biomass increases.

109 Based on this framework developed by Giletto et al. (2020), it is reasonable to expect that variation

110 in CNDC for potato would occur due to variation in total biomass and harvest index (i.e., timing

111 of tuber initiation, relative rate of tuber bulking) across $G \times E \times M$ gradients. Understanding the

112 effects of $G \times E \times M$ interactions on crop N requirements and status is critical to improving

113 agronomic outcomes and N use efficiency [NUE] within cropping systems (Lemaire & Ciampitti,

114 2020).

115 Previous development of CNDCs for potato (Duchenne et al., 1997; Bélanger et al., 2001a; Giletto

116 & Echeverría, 2015; Ben Abdallah et al., 2016) has been conducted using a non-uniform set of

117 statistical methods and with limited quantification of uncertainty in either the range of plausible

118    $\%N_c$ values or the fitted parameter values themselves. This makes it difficult to ascertain whether

119   observed differences in CNDCs result from underlying $G \times E \times M$ effects, are confounded by the

120   limitations of the statistical approach, or biased due to insufficient quantity or quality of

121   experimental data (e.g., unbalanced distribution of N limiting and non-N limiting observations).

122   The conventional approach to fit a CNDC consists of a two-step process: first, the critical points

123   from the relationship of $\%N_{Plant}$ as a function of biomass are selected using statistical criteria;

124   second, a negative exponential curve is fit to the subset of critical points using non-linear

125   regression. There are two commonly used statistical approaches to identify critical points: (1)

126   linear-plateau curve fit and (2) ANOVA and protected multiple comparison.

127   Using a linear-plateau curve to derive critical points was originally suggested by Justes et al.

128   (1994). This approach is rigorous and requires sufficient empirical data such that a linear-plateau

129   curve can be identified (i.e., at least one N limiting and at least two non-N limiting data points) for

130   each observation date. Therefore, this approach can be difficult or impossible to implement due to

131   potential limitations of the experimental data used such as insufficient levels of N treatments (i.e.,

132   fewer than three treatment levels) or interactions between management practices and

133   environmental conditions (i.e., all observations are either N limiting or non-N limiting).

134   In contrast, many studies use methods similar to Ben Abdallah et al. (2016) where critical points

135   are determined using a simplified statistical method. In this approach, ANOVA is first used to

136   identify experimental dates where variation in biomass is statistically significant. Subsequently, a

137   protected multiple comparisons analysis is used to identify which experimental treatments had the

138   highest level of biomass – the treatment level with the significantly greatest level of biomass is

139   then defined as the critical point. While this statistical method is more flexible to implement, it

140 cannot resolve deficiencies in the underlying empirical data (e.g., insufficient level of N

141 treatments, interactions with environmental conditions) that the linear-plateau method was

142 designed to discriminate against. Therefore, the critical points selected using the simplified method

143 may be biased due to inherent deficiencies of the underlying experimental data used.

144 Novel statistical methods developed first by Makowski et al. (2020) provide a framework which

145 allows for standardization in statistical approach and quantification of uncertainty for deriving in

146 CNDCs which enables comparison of $\%N_c$ across $G \times E \times M$ interactions. In short, this framework

147 implements a hierarchical Bayesian model which simultaneously identifies critical points using

148 the linear-plateau method (e.g., Justes et al. (1994)) while fitting the negative exponential curve

149 which defines $\%N_c$. The advantage of this method is that it fits the CNDC from the entire set of

150 experimental data for a given $G \times E \times M$ interaction level and removes the arbitrary intermediate

151 step of separately identifying critical points. This approach has already been successfully used by

152 Ciampitti et al. (2021), Yao et al. (2021), and Fernández et al. (2021) to evaluate differences in

153 CNDCs across $G \times E \times M$ interactions for maize, wheat, and tall fescue cropping systems,

154 respectively. Through this single-step process, the Bayesian hierarchical method both eliminates

155 the need to separately identify critical points and implements the theoretically preferred method

156 (e.g., linear-plateau curve fit) to select critical points.

157 The Bayesian hierarchical method, however, remains subject to inferential bias due to both limited

158 quantity and quality of experimental data (Fernández et al., 2021; Fernandez et al., 2022). With

159 respect to quantity, having an insufficient number of observations from a limited number of

160 experimental trials to derive an individual CNDC will result in increased bias in $\%N_c$. With respect

161 to quality, using experimental data that does not reflect a full range of biomass values or does not

162 sufficiently represent both limiting and non-limiting N conditions will result in increased bias in

163 %N_c. Datasets used to derive the CNDC using the Bayesian hierarchical method should contain at

164 least eight experimental trials containing at least three N treatments and at least three sampling

165 dates (Fernández et al., 2022).

166 However, there are multiple approaches to pooling across G × E × M interactions within the

167 Bayesian hierarchical method to address this bias due to experimental data limitations: no pooling,

168 full pooling, and partial pooling.

169 The no pooling approach treats each experimental data level independently where experimental

170 data from one level is not used in inference for any other level (McElreath, 2020). The no pooling

171 approach was used by Makowski et al. (2020), Ciampitti et al. (2021), Yao et al. (2021), and

172 Fernández et al. (2021) to develop independent models for each G × E × M interaction. For the

173 Bayesian hierarchical method, the no pooling approach is directly limited by the quantity and

174 quality of experimental data for each G × E × M interaction level.

175 The full pooling approach, in contrast, treats each experimental data level in an equivalent manner

176 where the experimental data from all levels are used simultaneously for inference (McElreath,

177 2020). The full pooling approach was used by Fernández et al. (2021) to develop a single model

178 across G × E × M interaction levels. While this approach was found by Fernández et al. (2021) to

179 potentially reduced inferential bias from the Bayesian hierarchical method (i.e., by increasing the

180 combined quantity and quality of data used to fit a given CNDC), the fully pooled approach has

181 the explicit tradeoff that inference at individual levels of G × E × M interactions is not possible.

182 The partial pooling approach balances the tradeoffs between fitting a single population-level model

183 (i.e., full pooling) and fitting multiple independent group-level models (i.e., no pooling) by using

184 the entire set of experimental data to fit a single model with where the data from all other levels of

185 an effect influence the inference for a particular level and reduce inferential bias (McElreath,

186 2020). In this manner, individual effect levels are said to be "borrowing strength" through the

187 process of "shrinkage", where more extreme values are pulled toward the average (Lindstrom &

188 Bates, 1990; Bates, 2010). Therefore, using a partially-pooled Bayesian hierarchical method

189 should reduce both reduce the inferential bias for a given $G \times E \times M$ interaction level where the

190 quantity and quality of experimental data are not otherwise sufficient and enable inference for each

191 individual $G \times E \times M$ interaction level. However, the partial pooling approach has not yet been

192 implemented within in the Bayesian hierarchical method to derive CNDCs.

193 Building upon previous work, the objectives of this study are to 1) develop CNDCs using the

194 hierarchical Bayesian framework for potato varieties in Minnesota (from both previously

195 published and unpublished experimental data) and for potato varieties in Argentina (Giletto &

196 Echeverría, 2015), Canada (Bélanger et al., 2001a), and Belgium (Ben Abdallah et al., 2016) (from

197 previously published experimental data), 2) extend the implementation of the hierarchical

198 Bayesian framework using a partial pooling approach to compare CNDCs across $G \times E \times M$

199 interactions based on the uncertainty in $\%N_c$ and curve parameters a and b, 3) identify the optimal

200 methods to determine uncertainty in $\%N_c$ for use in calculating NNI and other derivative metrics,

201 and 4) compare CNDCs developed with the hierarchical Bayesian framework methods to

202 previously published CNDCs for the same data with different statistical methods.

203 **2. Materials and Methods**

204 *2.1. Experimental Data*

205 This study combines experimental data from both newly reported and previously published sources

206 (Ben Abdallah et al., 2016; Giletto et al., 2020). The data used for analysis in this study are

207 summarized in Table 1 and the relevant methods related to the experimental trials are reported

208 below. All individual experimental observations used in this study are presented in the

209 Supplemental Materials (Table S1).

Table 1. Summary of experimental data used in this study.

Study	Location	Variety	Site-Years	Sampling Dates	Samples
Present Study	Minnesota	Clearwater	2	10	30
		Dakota Russet	2	14	70
		Easton	2	14	70
		Russet Burbank	9	52	328
		Umatilla Russet	2	10	30
Giletto et al. (2020)	Argentina	Bannock Russet	3	13	52
		Gem Russet	4	18	72
		Innovator	4	18	72
		Markies Russet	2	9	36
		Umatilla Russet	3	14	56
	Canada	Russet Burbank	4	30	104
		Shepody	4	30	105
Ben Abdallah et al. (2016)	Belgium	Bintje	17	49	238
		Charlotte	7	24	114

210

211 2.1.1. Newly Reported Data – Minnesota

212 Six individual plot-scale field experiments were conducted over a total of eight years (MN-1:

213 1991–1992; MN-2: 2014-2015, MN-3: 2016, MN-4: 2018-2019, MN-5: 2019, MN-6: 2020) on

214 irrigated plots at the Sand Plain Research Farm [SPRF] in Becker, MN (45º 23' N, 93º 53' W)

215 (Table 2). The soil is characterized as a Hubbard loamy sand (Sandy, mixed, frigid Entic

216 Hapludolls) with organic matter content ranging from 1.3 to 2.5% and is excessively well drained

217 with low available water holding capacity (Hansen & Giencke, 1988; USDA NRCS, 2013). For a

218 typical growing season beginning on 1 May and ending on 15 September, mean temperature is

219 18.9ºC, cumulative precipitation is 383 mm, cumulative growing degree days are 1638 ºC days,

220 mean daily solar radiation is 22.7 MJ m^{-2}, and mean diurnal temperature difference is 11.6 ºC

221 based on a historical climate reconstruction for the period of 1980-2016 (Gelaro et al., 2017;

222 Weather Spark, 2021).

223

Table 2. Summary of newly reported experimental small-plot trials in Minnesota, USA.

Experiment	Year	Reference
MN-1	1991-1992	Rosen et al. (1992); Rosen et al. (1993); Errebhi et al. (1998)
MN-2	2014-2015	Sun (2017); Sun et al. (2019); Sun et al. (2020)
MN-3	2016	Crants et al. (2017)
MN-4	2018-2019	Gupta and Rosen (2019); Gupta et al. (2020); Li et al. (2021)
MN-5	2019	Bohman et al. (2020)
MN-6	2020	Rosen et al. (2021)

224

225 Apart from experimental N and variety treatments, all management and cultural practices were

226 managed by the staff at the SPRF in accordance with common practices for the region (Egel, 2017).

227 Nutrients were applied based on soil samples and University recommendations (Franzen et al.,

228 2018; Rosen, 2018), and supplemental irrigation was applied based on the University

229 recommended checkbook method (Wright, 2002; Steele et al., 2010). Additional details on

230 experimental procedures for these studies have been previously reported (Table 2).

231 A randomized complete block design with three or four replicates was used in each field

232 experiment. All studies evaluated at least 3 nitrogen rates (0 – 400 kg N ha^{-1}) for Russet Burbank

233 potato [*Solanum tuberosum* (L.)], with some studies evaluating additional potato varieties (Table

234 2). Nitrogen fertilizer was applied using various source and timing regimes including polymer

235 coated urea applied at planting and/or emergence, split-applied urea and urea-ammonium nitrate

236 at emergence and/or post-emergence, ammonium nitrate at planting, emergence, and/or post-

237 emergence. The maturity class of varieties evaluated in these experiments included: medium-late

238 – Clearwater and Dakota Russet; medium-late to late – Umatilla Russet; late – Easton; late to very

239 late – Russet Burbank (Thompson, 2013; Porter, 2014; Stark et al., 2020; OSU, 2021). Planting

240 density was 36,000 plants ha^{-1} for all experiments except for MN-1 which was planted at a density

241 of 48,000 plants ha^{-1}.

242 The experiments that evaluated multiple varieties had either a factorial design, or split-plot design

243 with variety treatment as the whole-plot and nitrogen treatment as the split-plot. Plots in these

244 studies were between 5.4 – 6.4 m wide (6 or 7 x 0.9 m rows) and 6.1 – 9.1 m long. Experiments

245 were planted each year in late-April to early-May and were mechanically harvested in mid-

246 September with vines terminated one to two weeks prior to harvest. A summary of N management

247 practices and varieties evaluated for each of these studies is given below (Table 3).

248

Table 3. Summary of experimental treatments evaluated in small-plot trials in Minnesota, USA.

Experiment	N treatments[†]	N rates [kg ha^{-1}]	Varieties
MN-1	10	0, 135, 180, 225, 270	Russet Burbank
MN-2	5	135, 200, 270, 335, 400	Russet Burbank, Dakota Russet, Easton
MN-3	4	45, 180, 245, 335	Russet Burbank
MN-4	3	135, 270, 400	Russet Burbank, Clearwater, Umatilla Russet
MN-5	8	45, 155, 245, 290, 335	Russet Burbank
MN-6	8	55, 155, 245, 270, 290, 335	Russet Burbank

[†] Including N source, timing, and placement combinations occurring at an equivalent N rate

249

250 Samples of vine biomass were harvested immediately prior to mechanical termination for

251 determination of fresh weight vine yield. Harvested tubers were mechanically sorted into weight

252 classes and graded (USDA, 1997), and fresh weight tuber yield was determined as the sum of all

253 weight classes and tuber grades. Harvested biomass was oven dried at 60ºC to determine dry matter

254 content of vines and tubers. Dry weight tuber and vine biomass was calculated as the product of

255 fresh weight and dry matter content for each tissue respectively. Total N concentration of vines

256 and tubers was determined from subsamples of plant tissues with either combustion analysis

257 (Elementar Vario EL III, Elementar Americas Inc., Mt. Laurel, NJ) using standard methods

258 (Horneck & Miller, 1998), or with the salicylic Kjeldahl method (Horwitz et al., 1970). Total N

259 content of vines and tubers was calculated as the product of N concentration and dry weight

260 biomass for each tissue respectively. Total plant N content [N_{Plant}] (kg N ha^{-1}) was calculated from

261 the sum of tuber and vine N content. Total plant dry weight biomass [W] (Mg dry wt. ha^{-1}) was

262 calculated from the sum of vine and tuber dry weight biomass. Plant N concentration [%N_{Plant}] (g

263 N 100 g^{-1} dry wt.) was calculated as the ratio of N_{Plant} to W.

264 Whole-plant samples were also regularly collected during the period of late-May to early-

265 September (Table 4). Two to three plants were harvested from each plot on four to six dates each

266 year with vines, roots, and tubers each measured separately. Dry weight biomass, N concentration,

267 and N content for vines and tubers were determined for these in-season plant tissue samples using

268 the methods described above. Calculations for W, N_{Plant}, and $\%N_{Plant}$ were the same as methods

269 previously described above.

270

Table 4. In-season and harvest sampling dates for the experimental small-plot trials in Minnesota, USA.

| Experiment | Year | In-Season | | | | | | Harvest |
		1	2	3	4	5	6	
MN-1	1991	12 June	24 June	2 July	16 July	30 July	13 Aug	10 Sept.
MN-1	1992	10 June	25 June	17 July	5 Aug.	26 Aug.		15 Sept.
MN-2	2014	30 June	15 July	24 July	11 Aug.	26 Aug.	8 Sept.	15 Sept.
MN-2	2015	23 June	7 July	21 July	4 Aug.	17 Aug.	1 Sept.	16 Sept.
MN-3	2016	28 June	13 July	26 July	3 Aug.	10 Aug.		13 Sept.
MN-4	2018	26 June	10 July	18 July	1 Aug.			13 Sept.
MN-4	2019	26 June	11 July	24 July	7 Aug			16 Sept.
MN-5	2019	25 June	9 July	23 July	6 Aug	21 Aug		16 Sept.
MN-6	2020	24 June	7 July	22 July	4 Aug			16 Sept.

271

272 2.1.2. Previously Published Data – Belgium, Argentina, and Canada

273 Experimental data reported in two previous studies, Giletto et al. (2020) and Ben Abdallah et al.

274 (2016), were included in the analysis conducted for the present study. The data from Giletto et al.

275 (2020) comprises two separate experimental data sets from Argentina (Giletto & Echeverría, 2015)

276 and Canada (Bélanger et al., 2000, 2001a, 2001b). All data from the Giletto et al. (2020) study

277 used in the present analysis was included in this previous publication.

278 In the Canadian study, two varieties (Russet Burbank and Shepody) and four N fertilization rates

279 (0, 50, 100, and 250 kg ha^{-1}) were evaluated under irrigated and non-water limiting conditions with

280 each variety having four site-years of experimental data and either seven or eight sampling dates

281 per site-year (Table 1). These small-plot experiments were conducted in the upper St. John River

282 Valley of New Brunswick, Canada (47º 03' N; 67º 45' W). Nitrogen fertilizer for all treatments

283 was ammonium nitrate applied at planting. The maturity class of varieties evaluated in these

284 experiments included: early to medium-early – Shepody; late to very late – Russet Burbank (Stark

285 et al., 2020; OSU, 2021). Planting density was 29,000 and 44,000 plants ha^{-1} for Russet Burbank

286 and Shepody, respectively. The soil texture for these experiments was classified as either loam or

287 clay loam with organic matter content ranging from 2.6 to 3.0%. For a typical growing season

288 beginning on 1 June and ending on 10 October, mean temperature is 15.7ºC, cumulative

289 precipitation is 371 mm, cumulative growing degree days are 1150 ºC days, mean daily solar

290 radiation is 19.1 MJ m^{-2}, and mean diurnal temperature difference is 10.0 ºC based on a historical

291 climate reconstruction for the period of 1980-2016 (Gelaro et al., 2017; Weather Spark, 2021).

292 In the Argentina study, five varieties (Bannock Russet, Gem Russet, Innovator, Markies Russet,

293 and Umatilla Russet) and four N fertilization rates (0, 80, 150, and 250 kg N ha^{-1}) were each

294 evaluated under irrigated and non-water limiting conditions for between two and four site-years

295 with between four and five sampling dates per site year (Table 1). These small-plot experiments

296 were conducted in Balcarce in the province of Buenos Aires, Argentina (37º 45' S; 58º 18' W).

297 Nitrogen fertilizer for all treatments was urea applied at planting. The maturity class of varieties

298 evaluated in these experiments included: early to medium – Innovator; medium to late – Gem

299 Russet; medium-late to late – Umatilla Russet; late to very late – Bannock Russet and Markies

300 Russet (Giletto & Echeverría, 2015; Stark et al., 2020; OSU, 2021). The planting density was

301 59,000 plants ha^{-1} for all varieties. Soil texture for these experiments was classified as a loam with

302 organic matter content ranging from 4.2 to 5.2%. For a typical growing season beginning on 10

303   October and ending on 10 March, mean temperature is 18.4ºC, cumulative precipitation is 428

304   mm, cumulative growing degree days are 1739 ºC days, mean daily solar radiation is 25.5 MJ m^{-}

305   ^{2}, and mean diurnal temperature difference is 13.6 ºC based on a historical climate reconstruction

306   for the period of 1980-2016 (Gelaro et al., 2017; Weather Spark, 2021).

307   The data from Ben Abdallah et al. (2016) represents multiple experimental data set from Belgium.

308   Only a portion of the data from the Ben Abdallah et al. (2016) study used in the present analysis

309   was included in this previous publication – while the dry weight biomass data were previously

310   reported, the N concentration data from the Ben Abdallah et al. (2016) experiment is reported for

311   the first time in this work.

312   In the Belgium studies, three to six N rates (ranging from 0 to 250 kg N ha^{-1}) were evaluated for

313   two varieties (Bintje and Charlotte) for 17 and 7 site-years, respectively, with between one and

314   eight sampling dates per site year (Table 1). These small-plot experiments were conducted in

315   Gembloux, Belgium (50º 33' N; 4º 43' E). Nitrogen fertilizer for all treatments was ammonium

316   nitrate applied at planting. The maturity class of varieties evaluated in these experiments included:

317   medium – Charlotte; late – Bintje (CFIA, 2013; AHDB, 2015; OSU, 2021). The planting density

318   was 38,000 plants ha^{-1} for all varieties. The soil texture for these experiments was classified as

319   loam, sandy loam, silt loam, or silty clay loam with organic matter content ranging from 1.3 to

320   2.6%. For a typical growing season beginning on 20 April and ending on 20 September, mean

321   temperature is 15.5ºC, cumulative precipitation is 244 mm, cumulative growing degree days are

322   1313 ºC days, mean daily solar radiation is 20.0 MJ m^{-2}, and mean diurnal temperature difference

323   is 8.3 ºC based on a historical climate reconstruction for the period of 1980-2016 (Gelaro et al.,

324   2017; Weather Spark, 2021).

325   A comparison of G (i.e., maturity class), E (i.e., soil texture, growing season weather conditions),

326   and M (i.e., planting density, source and timing of N fertilizer) factors across the G × E × M

327   interaction levels evaluated in this study is presented in Table 5.

328

Table 5. Comparison of key experimental factors including for Genotype [G]: variety maturity class [Maturity Class]; Environment [E]: soil texture classification [Soil Texture], soil organic matter content [OM], growing season mean daily temperature [T_{Mean}], growing season cumulative precipitation [Precip.], growing season mean diurnal temperature difference [$\Delta T_{Diurnal}$], growing season cumulative growing degree days [GDD], growing season mean daily incident solar radiation [Sol. Rad.]; and Management [M]: planting density [Density], and N fertilizer application source and timing.

		G	E							M	
Location	Variety	Maturity Class†	Soil Texture‡	OM [%]	T_{Mean} [°C]	Precip. [mm]	$\Delta T_{Diurnal}$ [°C]	GDD [°C d]	Sol. Rad. [MJ m⁻²]	Density [plants ha⁻¹]	N Source & Timing§
Argentina	Bannock Russet Gem Russet Innovator Markies Russet Umatilla Russet	L to VL M to L E to M L to VL ML to L	L	4.2 to 5.2	18.4	428	13.6	1739	25.5	59,000	Urea @ PL
Belgium	Bintje Charlotte	L M	SiCL, SiL, L, SL	1.3 to 2.6	15.5	244	8.3	1313	20.0	38,000	AN @ PL
Canada	Russet Burbank Shepody	L to VL E to ME	CL, L	2.6 to 3.0	15.7	371	10.0	1150	19.1	29,000 44,000	AN @ PL
Minnesota	Clearwater Dakota Russet Easton Russet Burbank Umatilla Russet	ML ML L L to VL ML to L	LS	1.3 to 2.5	18.9	383	11.6	1638	22.7	36,000	AN, Urea, UAN, and/or PCU @ PL, EM, and/or P-EM

† Early [E], medium-early [ME], medium [M], medium-late [ML], late [L], very late [VL]

‡ Silty clay loam [SiCL], clay loam [CL], silt loam [SiL], loam [L], sandy loam [SL], loamy sand [LS]

§ Ammonium nitrate [AN], urea-ammonium nitrate [UAN], polymer-coated urea [PCU], planting [PL], emergence [EM], post-emergence [P-EM]

331   *2.2.   Statistical Methods*

332   Based on the general approach outlined by Makowski et al. (2020), this study implemented a

333   partially-pooled Bayesian hierarchical framework to infer CNDC parameters for each location and

334   variety within location, assess the uncertainty in model parameters and $\%N_c$, and compare fitted

335   CNDCs across the effects of location and variety.

336   In summary, this statistical approach uses the entire set of experimental data (Figure 1a) and does

337   not require any preliminary or intermediary statistical analysis. At the level of each experimental

338   sampling date, a linear-plateau curve is fit for biomass as a function of N concentration (Figure

339   1b) and the join point of the linear-plateau curve is used to define the $\%N_c$. Simultaneously, a

340   negative exponential curve (i.e., CNDC) is fit across all experimental sampling dates for a given

341   effect level of the hierarchical model (e.g., location, variety) where the critical point of each linear-

342   plateau curve lies exactly upon the negative exponential curve (Figure 1b). In this manner, the

343   linear-plateau curve fitted for any given date is influenced by the data from all other experimental

344   sampling dates through the fitting of the negative exponential curve. In comparison, the

345   conventional statistical approach fits a negative exponential curve to the subset of critical points

346   (Figure 1c) which are identified via an intermediate statistical analysis (i.e., ANOVA and protected

347   multiple comparisons).

348
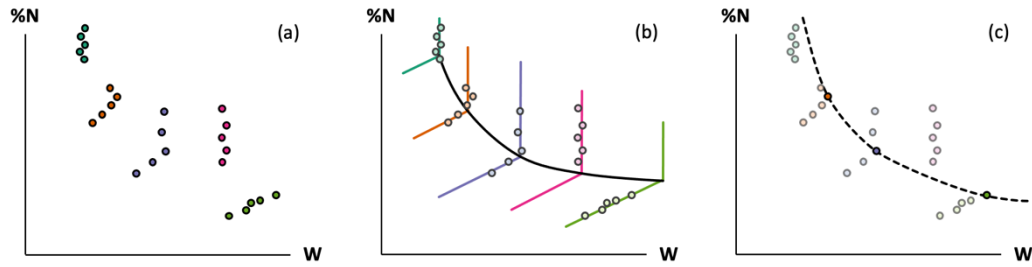
Figure 1. Hypothetical example comparing various statistical methods where plant N concentration [%N] as a function of biomass [W] on five experimental sampling dates for (a) raw experimental data, (b) linear-plateau curves (solid colored lines) fitted for each experimental sampling date (points for each date distinguished by color) and the critical N dilution curve (solid black line) fitted using the hierarchical Bayesian method based on Makowski et al. (2020), and (c) critical points (opaque) and non-critical points (transparent) selected using conventional statistical analysis (i.e., ANOVA and protected multiple comparison) with critical N dilution curve (dotted line) fitted using conventional methods (i.e., non-linear regression using only the critical points).

349

350   The Bayesian hierarchical framework outlined by Makowski et al. (2020) was extended to

351   explicitly include the $G \times E \times M$ interaction levels within the fitted model using a partial pooling

352   approach. Experimental data were nested according to location and variety within location, where

353   the linear-plateau curve fitted for each experimental sampling date is nested within a given level

354   of variety within location (Figure 2). This model structure leverages the advantages of partial

355   pooling to addresses the limitations identified by Fernández et al. (2021) that a sufficient quantity

356   and quality of experimental data are required while still enabling direct inference on the individual

357   $G \times E \times M$ interaction levels. Using *R* (R Core Team, 2021a), the *brms* package (Bürkner, 2017,

358   2018) was used to implement the statistical framework outlined by Makowski et al. (2020) with

359   the modifications as previously described (Figure 2). The *brms* package, an interface to *Stan*

360   (Carpenter et al., 2017), was chosen due to the ability to include group-level effects (i.e., random

361   effects) which allows for the fit of this particular partially-pooled Bayesian hierarchical model.

362   The *brms* package includes a user-friendly modeling language, robust documentation, and a

363   diverse set of tools to analyze and assess models.

364
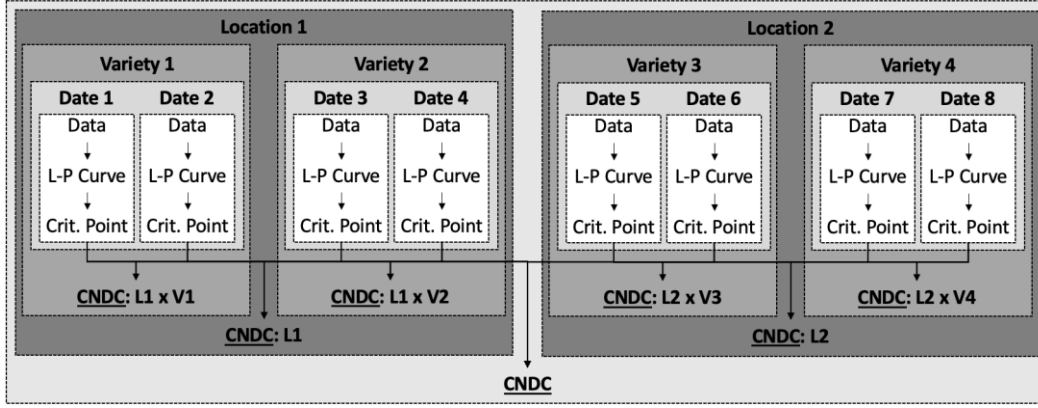
Figure 2. Flowchart showing nested structure used to fit critical N dilution curves [CNDC] using the hierarchical Bayesian method based on Makowski et al. (2020). Linear-plateau (L-P) curves and critical points (i.e., the fitted join point of each linear-plateau curve) are identified at the level of each experimental sampling date and pooled at various levels of location and variety within location to determine the CNDC for that level. This hierarchical model structure simultaneously fits all individual levels of location and variety within location, as well as for the global level of all experimental data, which allows for direct comparison across levels.

365

366 A non-linear *brms* model was defined by combining the two separate expressions used by

367 Makowski et al. (2020) to parameterize the Bayesian hierarchical model as previously

368 implemented with *rjags* (Plummer, 2019) and *JAGS* statistical software (Plummer, 2013).

369 The first expression from Makowski et al. (2020) represents the linear-plateau component:

370 $\text{W} = min(W_{Max,\text{i}} + S_\text{i} \cdot (\%\text{N}_{\text{Plant}} - \%\text{N}_\text{c}), W_{Max,\text{i}})$ [3]

371 where S_i and $W_{Max,\text{i}}$ are the slope of the linear-plateau curve and the maximum value of biomass

372 (i.e., plateau) for a given date [i], respectively, *min* represents the minima function (i.e., the plateau

373 component), and W, $\%\text{N}_{\text{Plant}}$, and $\%\text{N}_\text{c}$ have the same meaning as previously defined in this present

374 study. This linear-plateau curve is defined with N concentration as the independent variable and

375 biomass as the dependent variable and is written in point-slope form where the reference point

376 used is the critical point.

377 The second expression from Makowski et al. (2020) represents the CNDC component:

378     $\%N_c = a \, W_{Max,i}^{-b}$ [4]

379   where a and b are the parameters that define the negative exponential curve and $\%N_c$ and $W_{Max,i}$

380   have the same meanings as defined above.

381   Using algebraic substitution (i.e., for $\%N_c$), these two expressions (Eq. [3] and Eq. [4]) were

382   combined to produce following non-linear *brms* model formula:

383     $W \sim min(W_{Max,i} + S_i \, (\%N_{Plant} - (a \, W_{Max,i}^{-b})), \, W_{Max,i})$ [5]

384   Two group-level (i.e., random) effects were specified for this *brms* model to parameterize the

385   nested structure (Figure 2). First, the parameters S and W_{Max} included group-level effects to fit a

386   linear-plateau curve to each experimental sampling date:

387     $W_{Max} + S \sim 1 + (1 \mid index)$ [6]

388   where *index* represents the unique level of each experimental sampling date, nested within a given

389   level of variety within location. Second, the parameters a and b included group-level effects to fit

390   the CNDC:

391     $a + b \sim 1 + (1 \mid location) + (1 \mid location{:}variety)$ [7]

392   where *location* and *location:variety* represents the unique effect level for location and variety

393   within location, respectively.

394   The *brms* model was fitted using 4 chains and 10000 iterations with 3000 warmups per chain. The

395   priors for this model were chosen based on expert knowledge (i.e., previously reported values),

396   empirical observations (i.e., summary values from the data set), and the joint prior predictive

397   distribution (i.e., if a set of relatively uninformative priors led to biologically or physically

398 impossible predictions, the prior ranges were narrowed) (Schad et al., 2021). This is particularly

399 important for hyperparameters dealing with the standard deviation between groups in a

400 hierarchical model. A summary of the prior values used in this model is given below (Table 6).

401

Table 6. Priors used in fitting the hierarchical Bayesian model with brms.

Parameter	Distribution	Bounds	
		Lower	Upper
a	Normal (5.3, 0.1)	0	∞
$\sigma(a_{location})$	Normal (0.10, 0.02)	$-\infty$	∞
$\sigma(a_{location:variety})$	Normal (0.05, 0.01)	$-\infty$	∞
b	Normal (0.40, 0.01)	0	1
$\sigma(b_{location})$	Normal (0.05, 0.02)	$-\infty$	∞
$\sigma(b_{location:variety})$	Normal (0.02, 0.01)	$-\infty$	∞
$Wmax$	Normal (8.0, 0.1)	1	∞
$\sigma(Wmax_{index})$	Normal (7.0, 1.0)	$-\infty$	∞
S	Normal (6.0, 0.1)	0	∞
$\sigma(S_{index})$	Normal (1.0, 0.1)	$-\infty$	∞
σ	Student's t (3, 1.0, 0.1)	$-\infty$	∞

402

403 The entire statistical and data workflow used to generate this analysis is reproducible and available

404 via GitHub repository (https://github.com/bohm0072/bayesian-cndc-potato). The *renv* package

405 (Ushey, 2021) was used to document the computing environment utilized while conducting this

406 analysis to ensure code portability and reproducibility.

2.3. Evaluating Uncertainty

407

408 2.3.1. Critical N Dilution Curve Parameter Uncertainty

409 After the statistical model was successfully fit to the data (n=28,000 draws), values for parameters

410 *a* and *b* of the CNDC were reported at the 0.05, 0.50 (i.e., median) and 0.95 quantiles for the effect

411 levels of *location* and *location:variety* to determine the 90% credible interval for each parameter.

412 The correlation between values for parameters *a* and *b* was determined for each effect level of

413 *location:variety* using the fitted parameter values at the level of the individual draws.

2.3.2. Critical N Concentration Uncertainty

414

415   The %N_c for a set of discrete values of W between 1 Mg dry wt. ha^{-1} and the maximum observed

416   value of W in the experimental data set was calculated for each individual draw based on the fitted

417   values of parameters *a* and *b* for that draw. From the distribution of %N_c values, the 0.05, 0.50

418   (i.e., median) and 0.95 quantile values were identified for each effect level of *location:variety* to

419   determine the 90% credible region for %N_c. This approach makes maximal use of the jointly

420   estimated parameters contained in the posterior distribution.

421   To develop curves approximating the upper and lower boundaries of the 90% credible region for

422   %N_c (i.e., the 0.05 and 0.95 quantile values, respectively), a negative exponential curve of the

423   same form as the CNDC (i.e., $y = a\,x^{-b}$) was fit using *nls* (R Core Team, 2021b) to the set of data

424   previously identified as defining the boundaries of the 90% credible region (i.e., 0.05 and 0.95

425   quantile values). These curves approximating the upper and lower boundaries of the credible

426   region for the CNDC are respectively referred to as CNDC$_{up}$ and CNDC$_{lo}$, where parameters a_{up}

427   and b_{up} correspond to CNDC$_{up}$ and parameters a_{lo} and b_{lo} correspond to CNDC$_{lo}$.

428   Additionally, an estimate of the 90% credible region was calculated by using the boundary values

429   of the 90% credible interval of parameters *a* and *b*. The estimate for the upper boundary of the

430   credible region for %N_c was determined from the 0.95 quantile value for parameter *a* and 0.05

431   quantile value for parameter *b*; the estimate for the lower boundary of the credible region of %N_c

432   was determined from the 0.05 quantile value for parameter *a* and 0.95 quantile value for parameter

433   *b*. This approach does not account for the joint estimation of parameters offered by the Bayesian

434   approach; therefore, the paired combination for parameters *a* and *b* (i.e., 0.05 and 0.95 quantiles)

435   might not actually occur in the posterior distribution.

436 To compare the various methods described above, the difference in critical N concentration

437 [$\Delta\%N_c$] was calculated between the 0.50 quantile (i.e., median) value for $\%N_c$, designated as the

438 reference values (i.e., $\Delta\%N_c$ with constant value of zero), and the various methods to quantify

439 uncertainty (i.e., 90% credible region for $\%N_c$, $CNDC_{up}$ & $CNDC_{lo}$, and estimates of credible

440 region for $\%N_c$ using 90% credible interval for parameters *a* and *b*). In this manner, the $\Delta\%N_c$ for

441 each method to quantify uncertainty in $\%N_c$ can be directly compared.

2.3.3. Comparing Critical N Concentration across G $\times$ E $\times$ M Effects

443 Similar to the above methods, the $\%N_c$ for each draw was calculated across a set of discrete values

444 of W over the range of 1 Mg dry wt. ha^{-1} and the maximum observed value of W in the

445 experimental data set. At the effect level of *location:variety*, the difference between the $\%N_c$ for a

446 given comparison and reference CNDC (i.e., $\Delta\%N_c$) was calculated at each value of W. From this

447 computed set of $\Delta\%N_c$, the 0.05, 0.50 (i.e., median) and 0.95 quantile values were identified for

448 each effect level of *location:variety* to determine the 90% credible region for $\Delta\%N_c$. For a given

449 range of W values, the comparison curve considered to be not significantly different from the

450 reference curve if the $\Delta\%N_c$ values for the 0.05 and 0.95 quantile values of $\%N_c$ were respectively

451 less than and greater than zero (i.e., the 90% credible region for $\Delta\%N_c$ contains zero). In the case

452 where the 0.05 quantile value for $\Delta\%N_c$ was greater than zero, the comparison curve was

453 considered to have a significantly greater $\%N_c$ than the reference curve. In the case where the 0.95

454 quantile value for $\Delta\%N_c$ was less than zero, the comparison curve was considered to have a

455 significantly lower $\%N_c$ than the reference curve. To evaluate $\Delta\%N_c$ in the present study, the $\%N_c$

456 for a given effect level of *location:variety* was compared to all other levels, and this approach

457 allows for the direct evaluation of $\Delta\%N_c$ across G $\times$ E $\times$ M effects.

458   2.3.4.   Comparing Critical N Concentration across Statistical Methods

459   An analogous method was also used to compare the CNDCs fitted in the present study to the

460   CNDCs published in previous studies (i.e., Ben Abdallah et al. (2016); Giletto et al. (2020)).

461   Specifically, the previously published curves were evaluated to see if they fell within the 90%

462   credible region for the corresponding curve fitted with the hierarchical Bayesian method in the

463   present study. Using the determined credible region for the $\%N_c$, it is possible to identify the range

464   for which two CNDCs are significantly different. If the previously identified $\%N_c$ value falls

465   outside of the credible region for $\%N_c$ identified in this study, then the two curves are determined

466   to be significantly different over the range for which the previous value falls outside of the credible

467   region. This approach allows for direct evaluation of differences in $\%N_c$ for CNDCs developed

468   from the same set of data across various statistical methods.

469   **3.   Results**

470   *3.1.   Fitted Critical N Dilution Curve*

471   The posterior distribution of fitted values for CNDC parameters *a* and *b* are presented below

472   (Figure 3) showing the median value and 90% credible interval (i.e., 0.05 and 0.95 quantile values).

473   For parameter *a*, there was no significant difference for the effect of location at 90% credible

474   interval threshold (Figure 3a). Although Argentina has a numerically greater value of parameter *a*

475   (4.95) than the other three locations (4.74 – 4.77), these differences are not significant.

476   Additionally, the variation in parameter *a* for the variety within location effect is negligible and

477   not statistically significant (Figure 3a).

478
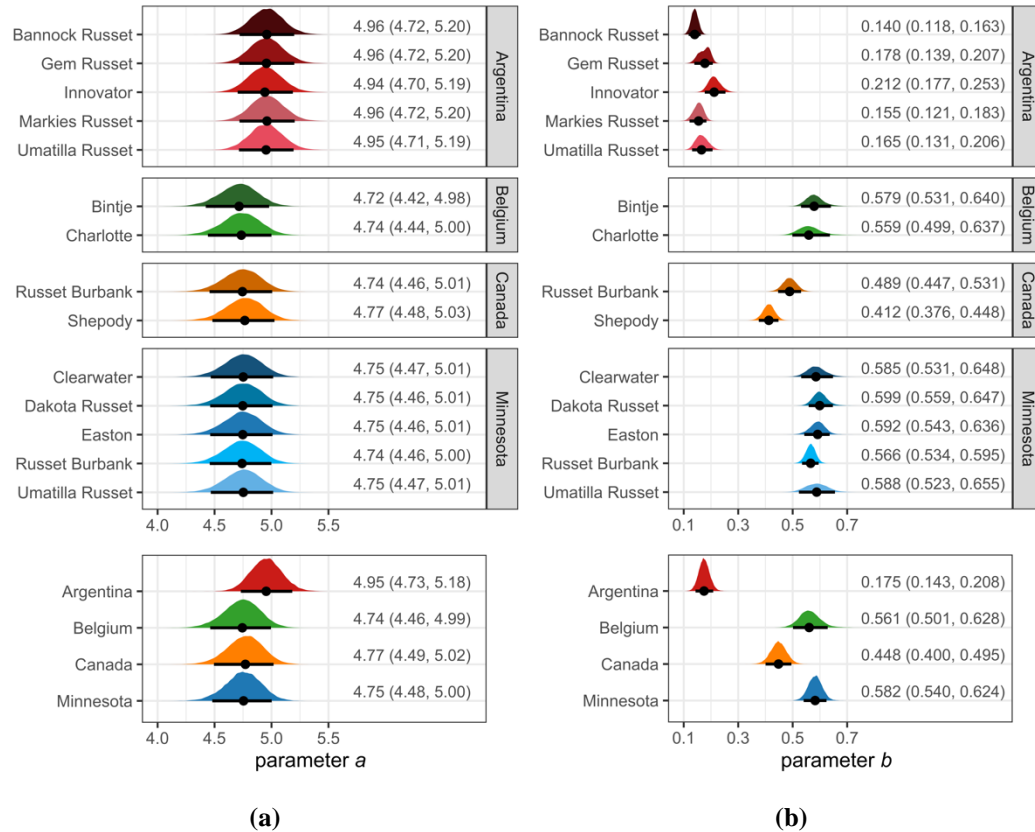
Figure 1. Posterior distribution of variety and variety within location effects for **(a)** parameter *a*; and **(b)** parameter *b*. Points represent median value and line represents 0.05 and 0.95 quantile range. Values displayed with the figures are the median value with the 90% credible interval boundaries (i.e., 0.05 and 0.95 quantiles) displayed within the parentheses.

479

480   For parameter *b*, there were significant differences for both the effect of location and variety within

481   location at a 90% credible interval threshold (Figure 3b). For location, Argentina had the lowest

482   value for parameter *b* (0.175), while Canada had a greater value for parameter *b* (0.448) than

483   Argentina but lower than either Belgium (0.561) or Minnesota (0.582). The difference between

484   parameter *b* for Belgium and Minnesota was not significant. For the variety within location effect,

485   parameter *b* significantly varied for varieties in Argentina and Canada, while there were no

486   significant differences in parameter *b* within either Belgium or Minnesota. For Argentina,

487   Innovator had the greatest value for parameter *b* (0.212), followed by Gem Russet, Umatilla

488   Russet, Markies Russet, and Bannock Russet (0.178, 0.165, 0.155, and 0.140, respectively). The

489 difference between Innovator and Umatilla Russet, Markies Russet, and Bannock Russet was

490 significant, while all other differences between varieties were not significant. For Canada, Russet

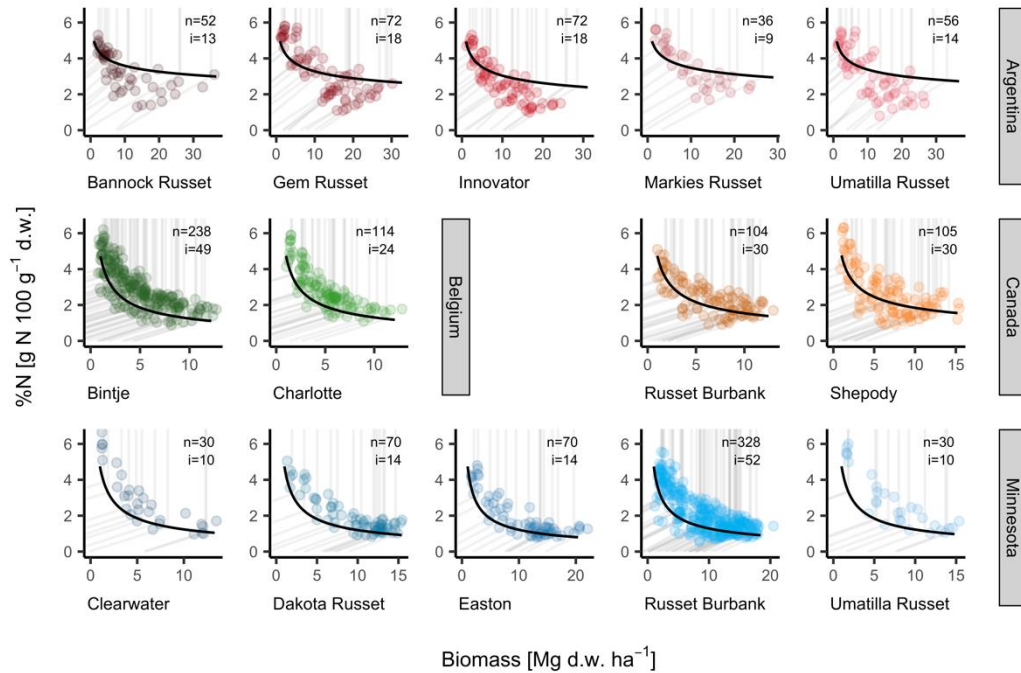491 Burbank had a significantly higher value for parameter *b* (0.489) than Shepody (0.412).

492 There was a positive correlation found between parameters *a* and *b* (Figure 4) which indicates that

493 quantifying differences in these parameter values independently (Figure 3) is not appropriate to

494 describe the uncertainty in %N_c determined by the correlated parameters. Stated alternatively,

495 significant differences for either parameter *a* or *b* do not necessarily imply that differences in %N_c

496 are also significant.

497
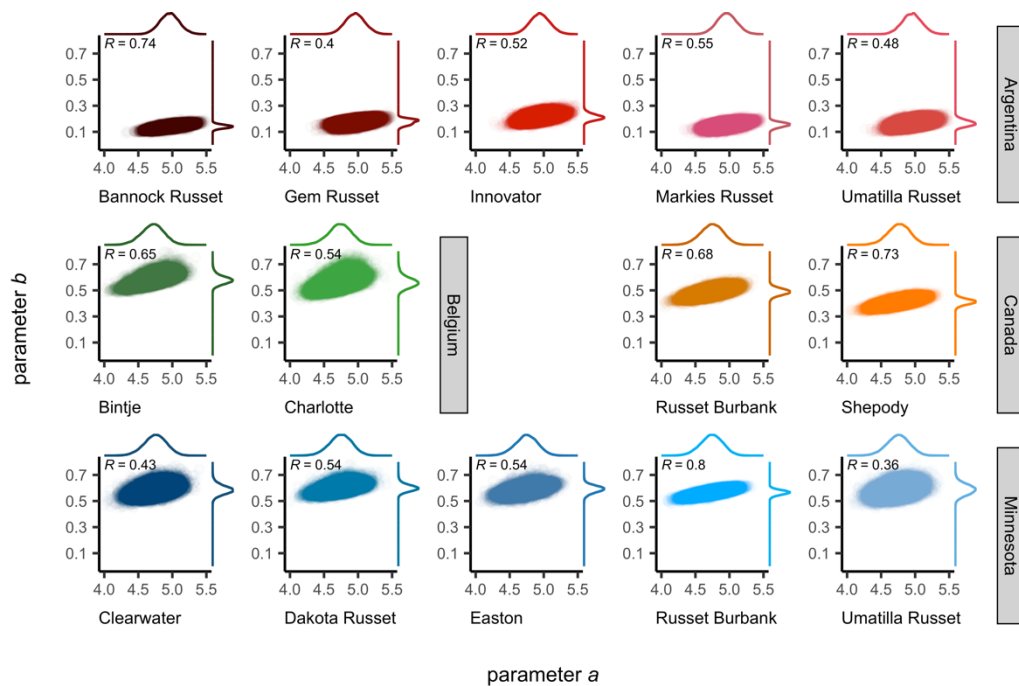
Figure 2. Distribution of posterior values for parameters *a* and *b* for each location within variety shown as a scatterplot with marginal density distribution given for each parameter. Pearson correlation coefficient [R] is displayed for the relationship between parameters *a* and *b*. Data are shown at the level of individual draws (n=28,000).

498

499 Critical N dilution curves for each variety within location and the experimental data, median linear-

500 plateau curve for each experimental sampling date, and median value of %N_c are presented (Figure

501   5). The individual linear-plateau curves fitted for each experimental sampling date nested within

502   each level of the variety within location effect are presented in the Supplemental Materials (Figure

503   S1).

504

Figure 3. Critical N dilution curves (i.e., median value of critical N concentration [%N_c]) fitted from the hierarchical Bayesian model are shown as a solid black lines for each variety within location. Biomass and N concentration [%N] data are displayed as points with the median linear-plateau curve for each sampling date shown as grey line. The number of samples [n] and the number of sampling dates [i] are displayed on each individual panel.

505

506   For the Argentina varieties, more than 60% of the observed data fall below the CNDC (i.e.,

507   represent N limiting conditions) with over 40% of sampling dates having exclusively N limiting

508   conditions observed. For both the Belgium and Minnesota varieties, more than 80% of the

509   observed data fall above the CNDC (i.e., represent non-N limiting conditions) with almost 30% of

510   sampling dates having exclusively non-N limiting conditions observed. For the Canada varieties,

511   over 60% of observed data represented non-N limiting conditions but less than 10% of sampling

512   dates had exclusively non-N limiting conditions observed (Figure S1).

513   *3.2.   Critical N Concentration Uncertainty*

514   The credible region for $\%N_c$ varies across variety within location and across levels of biomass

515   (Figure 6). The symmetry of the credible region distribution varies by variety within location.

516   Some levels of variety within location, such as Argentina $\times$ Gem Russet, have a skewed

517   distribution, while other levels, such as Canada $\times$ Shepody, have a symmetrical distribution (Figure

518   6a). There are also differences in the range of the credible region, where some varieties within

519   location, such as Argentina $\times$ Umatilla Russet, have greater uncertainty in $\%N_c$ than others, such

520   as Minnesota $\times$ Russet Burbank. The uncertainty in $\%N_c$ also varies across the level of biomass

521   for a given CNDC. For example, as the level of biomass increases, Argentina $\times$ Umatilla Russet

522   has an increasing credible region range, Minnesota $\times$ Russet Burbank has a decreasing credible

523   region range, and Argentina $\times$ Bannock Russet has a nearly constant credible region range.

524

(a)

(b)
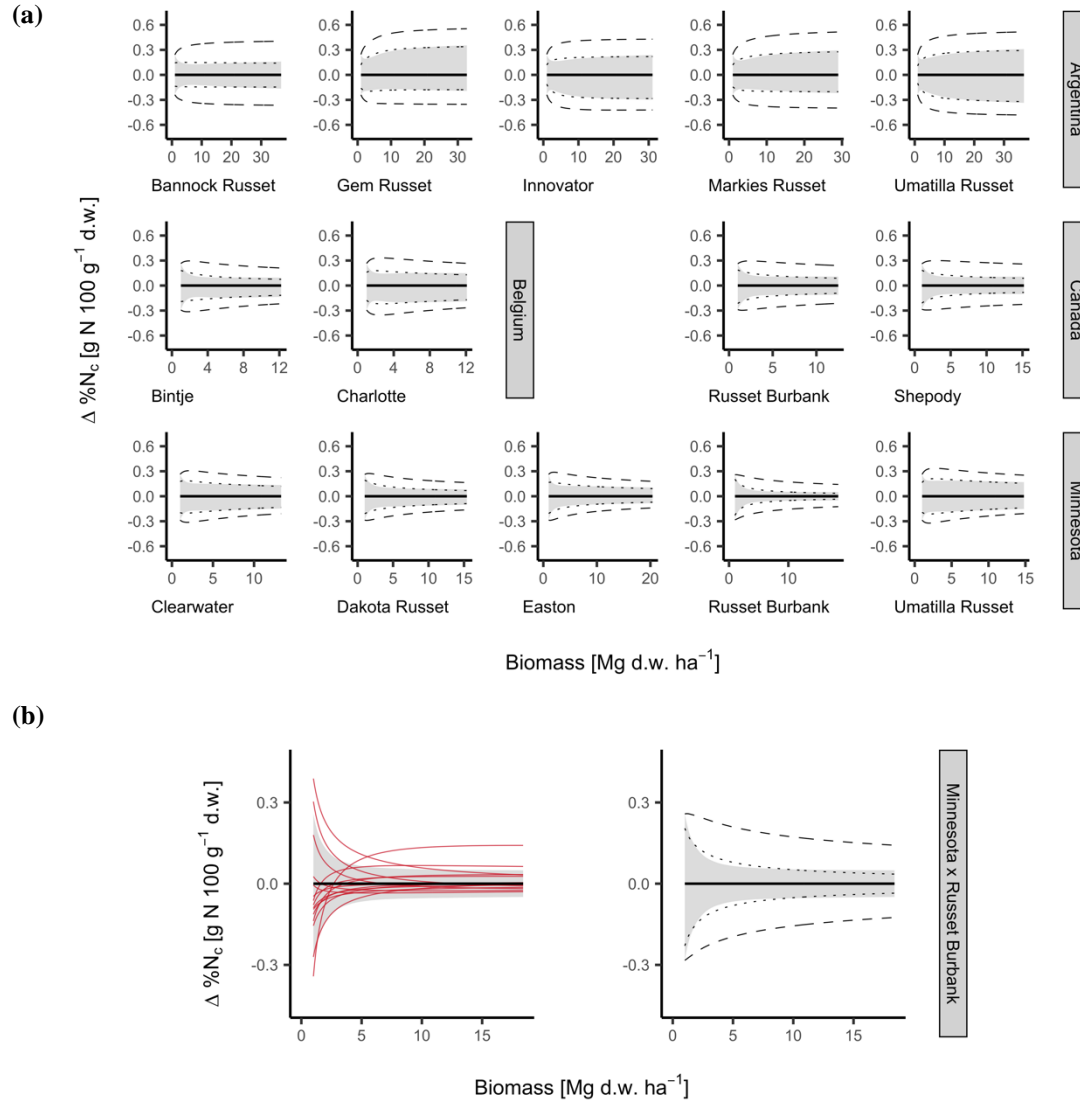
Figure 4. Comparison of the difference in critical N concentration values [$\Delta\%N_c$] between the median critical N concentration, represented as a solid black line at constant $\Delta\%N_c$ value of zero, and the various methods to quantify uncertainty in critical N concentration [$\%N_c$] where the magnitude of uncertainty in $\%N_c$ is equivalent the $\Delta\%N_c$ value. The grey shaded region represents the 90% credible region (lower bound, 0.05 quantile; upper bound, 0.95 quantile) for the fitted Bayesian hierarchical model. The dotted lines represent an estimation of the upper and lower bound of the 90% credible region from using the non-linear regression method (i.e., $CNDC_{lo}$ and $CNDC_{up}$). The dashed lines represent an approximation of uncertainty in $\%N_c$ based on the posterior distribution of critical N dilution curve [CNDC] parameters a and b. Data are presented for **(a)** all levels of variety within location, and **(b)** shown in greater detail for Minnesota × Russet Burbank only for individual draws from the Bayesian hierarchical model, for the non-linear regression method, and for the approximation of the 90% credible region based on the posterior distribution of parameters a and b. For **(b)**, the solid red line represents individual draws (n=15) from the posterior distribution of the fitted Bayesian hierarchical model.

525

Page 32

526   Estimation of the upper and lower boundaries of the 90% credible region using the non-linear

527   regression method (i.e., $CNDC_{lo}$ and $CNDC_{up}$) (Table 7) appears to be reasonable based on

528   graphical evaluation (Figure 6). However, these fitted $CNDC_{lo}$ and $CNDC_{up}$ curves do not

529   themselves represent a draw directly from the posterior distribution and do not necessarily

530   represent the most extreme possible curves (e.g., it is plausible to have an individual draw that

531   goes from the lower left to upper right corner of the interval, or vice versa) (Figure 6b). While

532   credible regions with boundaries that are non-monotonic (e.g., Argentina × Innovator) have

533   portions of the curve fit approximation that are poorer performing, the credible regions with

534   monotonic boundaries (e.g., Minnesota × Dakota Russet) seem to be satisfactory across the entire

535   range of the curve.

536

Table 1. Paired critical N dilution curve parameters for each variety within location for the median value (CNDC) from the posterior distribution of the fitted hierarchical Bayesian model and the estimates for the credible region lower ($CNDC_{lo}$) and upper ($CNDC_{up}$) boundaries using the non-linear regression method.

| Location	Variety	$CNDC_{lo}$		CNDC		$CNDC_{up}$	
		a_{lo}	b_{lo}	a	b	a_{up}	b_{up}
	Bannock Russet	4.82	0.146	4.96	0.140	5.10	0.135
	Gem Russet	4.80	0.190	4.96	0.178	5.07	0.152
Argentina	Innovator	4.83	0.241	4.94	0.212	5.06	0.193
	Markies Russet	4.82	0.167	4.96	0.155	5.08	0.135
	Umatilla Russet	4.85	0.195	4.95	0.165	5.06	0.143
Belgium	Bintje	4.52	0.606	4.72	0.579	4.90	0.567
	Charlotte	4.56	0.607	4.74	0.559	4.89	0.531
Canada	Russet Burbank	4.53	0.498	4.74	0.489	4.93	0.480
	Shepody	4.55	0.416	4.77	0.412	4.95	0.406
	Clearwater	4.56	0.622	4.75	0.585	4.93	0.558
	Dakota Russet	4.54	0.619	4.75	0.599	4.94	0.588
Minnesota	Easton	4.54	0.608	4.75	0.592	4.91	0.567
	Russet Burbank	4.51	0.562	4.74	0.566	4.95	0.567
	Umatilla Russet	4.56	0.631	4.75	0.588	4.92	0.546

537

538   However, the approximation of uncertainty in $\%N_c$ based directly on uncertainty in CNDC

539   parameters a and b, using the previously determined credible interval boundaries (Figure 3), were

540   found to contain the entire credible region for all varieties within location evaluated (Figure 6a).

541 Therefore, this approach directly using the uncertainty in CNDC parameters is quite uninformative

542 and should be used as a last resort to estimate $\%N_c$ uncertainty when the credible region defined

543 from either the original model fit or from the paired $CNDC_{lo}$ or $CNDC_{up}$ curves is unavailable. In

544 the absence of the credible region defined directly from the fitted hierarchical Bayesian model, the

545 $CNDC_{lo}$ and $CNDC_{up}$ (Table 7) are a suitable first-order representation of the credible region for

546 $\%N_c$.

3.3. Evaluating Differences between Critical N Concentration

3.3.1. Differences Related to $G \times E \times M$ Effects

549 While an evaluation of the pairwise differences between all varieties within location was

550 conducted and is presented in the Supplemental Materials (Figure S2), a subset of the results

551 comparing Minnesota $\times$ Russet Burbank to all other varieties within location, Argentina $\times$

552 Innovator to all other varieties within Argentina, Canada $\times$ Russet Burbank to all other varieties

553 within Canada, and Belgium $\times$ Bintje to all other varieties within Belgium are presented in detail

554 here (Figure 7).

555
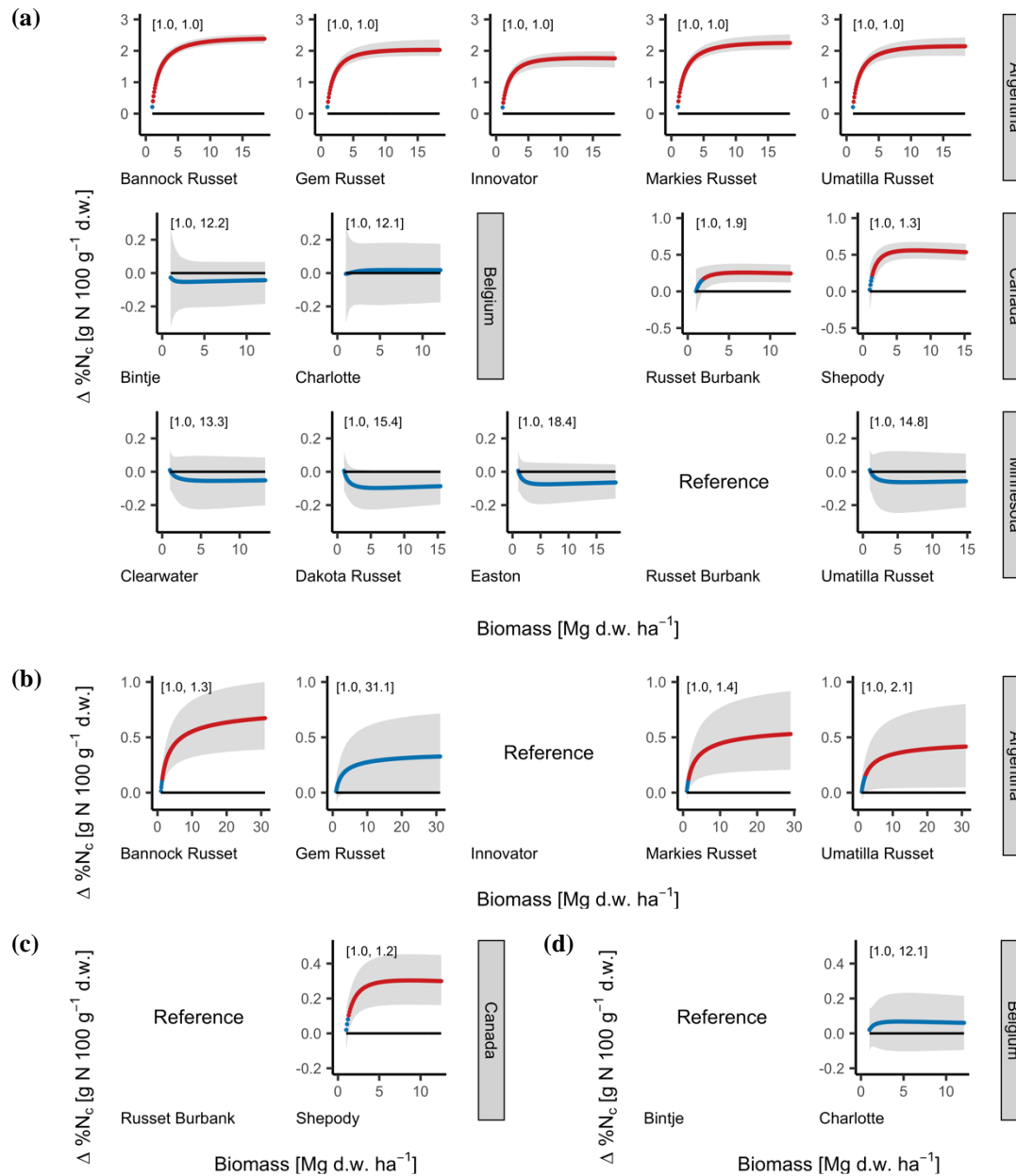
Figure 5. Comparison of the difference in critical N concentration values [$\Delta\%N_c$] between **(a)** Minnesota × Russet Burbank and all other varieties within location, **(b)** Argentina × Innovator and all other varieties within Argentina, **(c)** Canada × Russet Burbank and all other varieties within Canada, and **(d)** Belgium × Bintje and all other varieties within Belgium for critical N concentration [$\%N_c$] determined by the hierarchical Bayesian method. The grey shaded region represents the 90% credible region (lower bound, 0.05 quantile; upper bound, 0.95 quantile) for $\Delta\%N_c$. The colored points represent the median value for $\Delta\%N_c$ at a given Biomass level where blue or red color respectively indicate that the credible region for $\Delta\%N_c$ does or does not contain zero. The solid black line at constant $\Delta\%N_c$ value of zero represents $\%N_c$ for the reference curve (i.e., Minnesota × Russet Burbank, Argentina × Innovator, Canada × Russet Burbank, and Belgium × Bintje). The range of biomass values for which $\Delta\%N_c$ is not significantly different (i.e., credible region contains zero) is given in brackets.

556

557   For Minnesota × Russet Burbank, there were no significant differences in %N_c for any level of W

558   evaluated with any of the other varieties in Minnesota (i.e., Clearwater, Dakota Russet, Easton,

559   and Umatilla Russet) or with the Belgium varieties (i.e., Bintje, and Charlotte) (Figure 7a). The

560   %N_c values for both of the Canadian varieties (i.e., Russet Burbank, and Shepody) were

561   significantly greater than that for Minnesota × Russet Burbank when biomass values were greater

562   than 2 Mg ha^{-1} dry wt. The %N_c for Canada × Russet Burbank and Canada × Shepody were up to

563   0.3 and 0.6 g N 100 g^{-1} dry wt. greater than that for Minnesota × Russet Burbank, respectively.

564   The %N_c for the Argentina varieties (i.e., Bannock Russet, Gem Russet, Innovator, Markies

565   Russet, and Umatilla Russet) were significantly greater than for Minnesota × Russet Burbank,

566   except at a biomass value of 1.0 Mg dry wt. ha^{-1}, with a difference in value depending on variety

567   of up to 2.4 g N 100 g^{-1} dry wt.

568   For Argentina × Innovator, %N_c was significantly lower than for Argentina × Bannock Russet,

569   Argentina × Markies Russet, and Argentina × Umatilla Russet but was not significantly different

570   from Argentina × Gem Russet (Figure 7b). The %N_c values for Argentina × Bannock Russet,

571   Argentina × Markies Russet, and Argentina × Umatilla Russet were up to 0.5 g N 100 g^{-1} dry wt.

572   greater than that for Argentina × Innovator. For Canada × Russet Burbank, %N_c was significantly

573   lower than for Canada × Shepody (Figure 7c), with a difference in %N_c of up to 0.3 g N 100 g^{-1}

574   dry wt. For Belgium × Bintje, %N_c was not significantly different from Belgium × Charlotte

575   (Figure 7d).

576   There are two notable findings to point out. First, there were no significant differences between

577   Minnesota × Russet Burbank and any other varieties evaluated in Minnesota or between Belgium

578   × Bintje and Belgium × Charlotte. This finding did not hold true for all varieties within location

579   evaluated, however; Significant differences between varieties were found for both Argentina and

580 Canada. Second, the comparison between the Minnesota × Russet Burbank and Canada × Russet

581 Burbank curves as well as the comparison between the Minnesota × Umatilla Russet and Argentina

582 × Umatilla (Figure S2) were both significantly different.

583 3.3.2. Differences Related to Statistical Methods

584 When comparing the curves fit in the present study with the Bayesian hierarchical method to the

585 curves fit in the previous studies using conventional statistical methods, there were significant

586 differences between statistical curve fit methods for all varieties within location evaluated (Figure

587 8). None of the previous CNDCs fall entirely within the credible region for the respective CNDCs

588 developed in the present study.

589
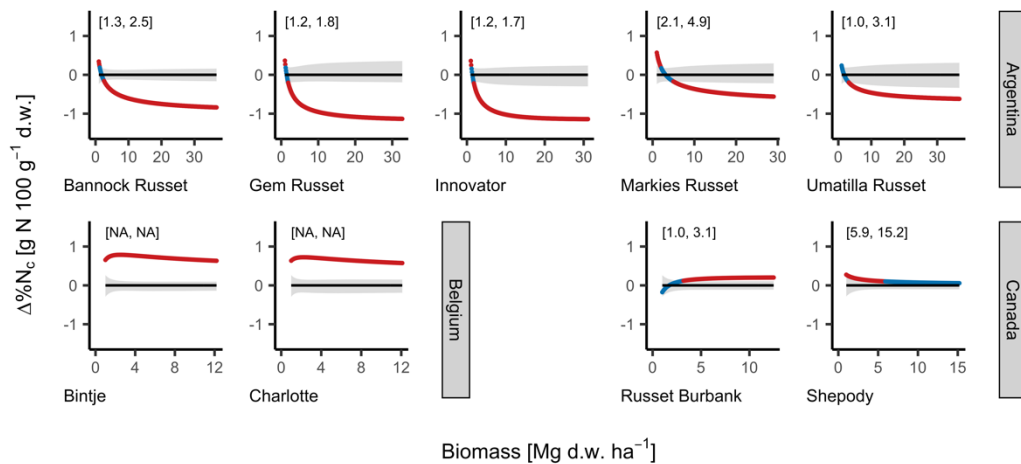
Figure 6. Comparison of the difference in critical N concentration values [$\Delta\%N_c$] between the conventional statistical methods used in previous studies (i.e., Argentina – Giletto and Echeverría (2015); Belgium – Ben Abdallah et al. (2016); Canada – Bélanger et al. (2001a)) and the hierarchical Bayesian method used in the present study for each variety within location. The grey shaded region represents the 90% credible region (lower bound, 0.05 quantile; upper bound, 0.95 quantile) for critical N concentration [$\%N_c$] from the hierarchical Bayesian method. The solid black line at a constant $\Delta\%N_c$ value of zero represents the median value for $\%N_c$ from the hierarchical Bayesian method. Red or blue points respectively indicate that $\Delta\%N_c$ falls outside of (i.e., is significant) or falls within (i.e., is not significant) the 90% credible region for $\%N_c$. The range of biomass values for which $\Delta\%Nc$ in not significant is given in brackets.

590

591 The $\%N_c$ values from the previously developed CNDCs for the Argentina varieties (Giletto &

592 Echeverría, 2015) were significantly less than that from the present CNDCs across all varieties for

593 biomass levels of greater 5 Mg dry wt. ha^{-1} (Figure 8). The magnitude of this difference was

594 relatively large, with the $\Delta\%N_c$ between the previous and present method ranging up to -0.6 to $-$

595 1.1 g N 100 g^{-1} dry wt., depending on variety. Therefore, relative to the statistical method used in

596 this study it appears that the statistical methods used by Giletto and Echeverría (2015) selected

597 biased critical points due to an overrepresentation of N limiting observations in the experimental

598 dataset (Figure 5, Figure S1) leading to a systematic underestimation of $\%N_c$.

599 The $\%N_c$ from the previously developed CNDCs for Belgium (Ben Abdallah et al., 2016) were

600 significantly greater than that from the CNDCs developed in the present study (Figure 8). For all

601 levels of biomass, $\Delta\%N_c$ between the previous and present methods was significantly different

602 with a value of 0.7 g N 100 g^{-1} dry wt. Therefore, relative to the statistical method used in this

603 study, it appears that the statistical methods used by Ben Abdallah et al. (2016) selected biased

604 critical points due to overrepresentation of non-N limiting observations in the experimental dataset

605 leading to a systematic overestimation of the $\%N_c$.

606 The $\%N_c$ from the previously developed CNDCs for Canada (Bélanger et al., 2001a) was

607 significantly greater for both Canada $\times$ Russet Burbank and Canada $\times$ Shepody than the present

608 CNDCs for biomass levels of less than 3 Mg dry wt ha^{-1} and greater than 6 Mg dry wt ha^{-1},

609 respectively (Figure 8). Relative to the other locations, however, the CNDCs for Canada were the

610 most similar between statistical methods, with a small value for $\Delta\%N_c$ of only 0.2 g N 100 g^{-1} dry

611 wt. Therefore, relative to the statistical method used in this study, it appears that the statistical

612 method used by Bélanger et al. (2001a) did not select biased critical points likely due to the

613 minimal bias observed in this experimental dataset.

614 Because a CNDC using the conventional statistical methods has not been previously published for

615 potato in Minnesota, no comparison across statistical methods is made for this experimental

616 dataset. However, the bias observed in the Minnesota experimental dataset is similar to the bias

617 found in the Belgium experimental dataset; therefore, using the conventional statistical methods

618 to derive a CNDC for Minnesota would likely overestimate $\%N_c$ relative to the hierarchical

619 Bayesian method.

620 **4. Discussion**

621 *4.1. Mechanisms of Dilution*

622 While the present study presents direct evidence of significant differences between CNDCs for

623 potato across $G \times E \times M$ effects, previous studies help describe the potential physiological

624 mechanisms for this source of variation. Reviewing previous work on this topic, Lemaire et al.

625 (2019) described a framework with which to consider the variation in relative partitioning of dry

626 matter. First, relative partitioning varies as biomass varies over the growing season indicating that

627 there is an ontogentic relationship between harvest index and biomass. Second, the allometric

628 trajectory of relative allocation (e.g., harvest index at a given level of biomass) is subject to

629 variation in non-ontogenetic factors (i.e., $G \times E \times M$ interactions).

630 The findings of Giletto et al. (2020) suggest that the variation in CNDCs for potato are due to non-

631 ontogenetic factors. In general, $G \times E \times M$ interactions that result in greater and more rapid relative

632 partitioning of biomass from vines (i.e., high N metabolic and structural tissue) to tubers (i.e., low

633 N storage tissues) will result in greater N dilution (i.e., lower $\%N_c$) at the same level of total plant

634 biomass (Lemaire et al., 2019). The two factors described by Giletto et al. (2020) affecting N

635 dilution due to non-ontogenetic factors are total plant biomass at tuber initiation (i.e., timing of

636 tuber initiation) and relative rate of tuber growth to plant growth (i.e., relative rate of tube bulking).

637 These two factors are affected by various physiological mechanisms and $G \times E \times M$ interactions;

638 however, relatively limited work has been conducted to comprehensively evaluate the combined

639 effect of $G \times E \times M$ interaction on these two physiological mechanisms for potato.

640 4.1.1. Timing of Tuber Initiation

641 The timing of tuber initiation is affected primarily by variety maturity class (i.e., G). Potato

642 varieties are classified on a spectrum of growth patterns where early maturing varieties are

643 considered to be determinate and later maturing varieties are considered to be indeterminate

644 (Thornton, 2020). Compared to indeterminate varieties, determinate varieties progress more

645 quickly to the tuber initiation growth stage (i.e., at lower total plant biomass) and have a more

646 rapid tuber bulking (i.e., biomass increase) with limited additional canopy and vine biomass

647 growth (i.e., increased harvest index for a given level of biomass) (Kleinkopf et al., 1981).

648 Therefore, it is expected that increasing earliness of maturity for a potato variety would result in

649 an increase in N dilution.

650 In the present study, differences in maturity class between resulted in differences in $\%N_c$. For

651 example, Argentina $\times$ Innovator, which has an early to medium maturity class, had significantly

652 lower $\%N_c$ than Argentina $\times$ Bannock Russet, Argentina $\times$ Markies Russet, and Argentina $\times$

653 Umatilla Russet, which have either a medium-late to late or late to very late maturity class;

654 however, Argentina $\times$ Gem Russet, which has a medium to late maturity class did not have a

655 significantly different $\%N_c$ from Argentina $\times$ Innovator (Table 7). This finding supports the

656 hypothesis that varieties with an earlier maturity class (i.e., earlier tuber initiation) will have lower

657 $\%N_c$ (i.e., greater N dilution).

658 Timing of tuber initiation is also subject to $G \times E \times M$ interactions. Ideal conditions for tuber

659 initiation are moderate to low soil N availability, shorter day length, high light intensity, and cool

660 nighttime temperatures (Ewing & Struik, 1992; Thornton, 2020); when N fertilizer management

661 results in excessively high soil N availability (Kleinkopf et al., 1981), under conditions of reduced

662 solar irradiance (Menzel, 1985), or when nighttime soil temperature are elevated (Slater, 1968;

663 Kim & Lee, 2019), tuber initiation can be delayed. Therefore, both M effects that result in

664 excessive early-season soil N availability (e.g., all N applied at planting in a soluble form) and E

665 effects that result in increased solar irradiance or reduced nighttime temperatures (i.e., increased

666 diurnal temperature difference) could result in an increase in N dilution.

667 However, due the limitation of the experimental studies (i.e., the effect of M was not systematically

668 varied across a given G x E interaction), it is not possible to directly assess the impact of diurnal

669 temperature difference, solar radiation, or N fertilizer source and timing (Table 5) on the timing of

670 tuber initiation and N dilution distinct from the combined effect of G x E x M interactions.

671 4.1.2. Rate of Tuber Bulking

672 The rate of tuber bulking and allocation of biomass to tubers is subject to the effects of E.

673 Conventionally, potential biomass production has been considered as the product of total solar

674 radiation and radiation use efficiency (Monteith, 1977; Sinclair & Muchow, 1999) as has been

675 successfully applied to potato (Allen & Scott, 1980). Previous studies have suggested that

676 decreasing diurnal temperature difference results in a reduction in tuber bulking rate (i.e., radiation

677 use efficiency), most likely as a result of increasing utilization of photosynthesis assimilates for

678 maintenance (via increased respiration) as nighttime temperature increases (Benoit et al., 1986;

679 Bennett et al., 1991; Lizana et al., 2017); however, Kim & Lee (2019) did not observe any effect

680 of increasing diurnal temperature difference on tuber bulking rate.

681 Given the limitation of the experimental studies (i.e., the effect of E was not systematically varied

682 across a given G x M interaction), it is not possible to directly assess the impact of diurnal

683 temperature difference and solar radiation (Table 5) on the rate of tuber bulking across G x E x M

684 interactions.

685 Planting density is an important effect of M that may play a key role in determining the relative

686 partitioning of biomass for to tuber. Previous studies investigating this effect have found that as

687 planting density increases, leaf area index increases (Bremner & Taha, 1966; Ifenkwe & Allen,

688 1978; Allen & Scott, 1980), tuber dry weight biomass on a per area basis increases (Bremner &

689 Taha, 1966; Ifenkwe & Allen, 1978), while tuber dry weight biomass on a per plant basis decreases

690 (Bremner & Taha, 1966; Ifenkwe & Allen, 1978). The combination of the effect of increasing

691 planting density could plausibly result in the net effect of an increased relative proportion of

692 biomass allocated to vines (i.e., reduction in harvest index) (Vander Zaag et al., 1990), therefore

693 reducing N dilution and resulting in an increased $\%N_c$.

694 In the present study, variations in $\%N_c$ due to variation in planting density were observed. For

695 example, Argentina has the highest planting density of any location (Table 5) which resulted in

696 greater $\%N_c$ than all other locations (Figure S2). The relative effect of planting density also appears

697 to be of greater magnitude than other sources of variation (e.g., maturity class). For example,

698 Canada × Russet Burbank, which has a late to very late maturity class and planting density of

699 29,000 plants ha^{-1}, had a lower $\%N_c$ than Canada × Shepody, which has an early to medium-early

700 maturity class and planting density of 44,000 plants ha^{-1} (Table 5, Figure 7c). Therefore, this

701 finding suggests that the effect of planting density (i.e., rate of tuber bulking) may be relatively

702 more important at controlling %N_c than the effect of maturity class (i.e., timing of tuber initiation).

703 Because there was only a single level of M (e.g., planting density) within each level of G $\times$ E for

704 the experimental trials considered here, additional experimentation is required to fully consider the

705 independent effects of G, E, and M on critical N dilution. Therefore, future experimental studies

706 explicitly investigating the effect of M (e.g., planting density) on %N_c should be conducted to

707 properly consider the combined effects the G $\times$ E $\times$ M interaction.

708 4.1.3. Comparison to Other Crops

709 These findings contrast somewhat with the previous studies evaluating G $\times$ E $\times$ M effects on %N_c.

710 Yao et al. (2021) found a similar magnitude of effect on %N_c for both G and E effects for wheat

711 in China; however, Yao et al. (2021) also reported an E effect where %N_c for wheat in China was

712 significantly different from that reported by Makowski et al. (2020) for wheat in France. Ciampitti

713 et al. (2021) identified variation in %N_c for maize as a result of G $\times$ M interactions due to variation

714 in hybrid and planting density. Fernández et al. (2021) found that variation in %N_c for tall fescue

715 across G $\times$ E $\times$ M effects was negligible. In any case, the magnitude of the difference in %N_c

716 across G x E x M interactions reported by the previous studies for wheat, maize, and tall fescue

717 (Makowski et al., 2020; Ciampitti et al., 2021; Fernández et al., 2021; Yao et al., 2021) is less than

718 that was observed in the present study for potato.

719 Therefore, the impact of G $\times$ E $\times$ M on %N_c is not only significant for potato, but is also of

720 potentially of much greater relative importance compared to other crops (e.g., wheat, maize, tall

721 fescue). This is because the magnitude of variability in %N_c due to G $\times$ E $\times$ M interactions found

722 in the present study is relatively greater for potato than other crops; however, further additional

723 experimental data are needed to confirm that this finding is not an artifact of the statistical methods

724 or limitations of experimental data used in the present study.

725 *4.2. Implication of G × E Variation on N Use Efficiency*

726 Understanding and properly interpreting the impact of G × E × M effects on NUE is a critical goal

727 necessary to improve N fertilizer use; however, this must be done while controlling for the effect

728 of crop N status (Lemaire & Ciampitti, 2020). The previous findings of Bohman et al. (2021)

729 demonstrated that interpreting NUE and its constituent component of N utilization efficiency

730 [NUtE] is directly related to the parameters of the CNDC through the critical N utilization

731 efficiency curve [CNUtEC] which defines the critical value of NUtE [NUtE$_c$]:

732 $\text{NUtE}_c = 1000 \, (10 \, a \, W^{-b})^{-1}$ [8]

733 where parameters *a* and *b*, and W have the same meaning and units as previously defined in the

734 present study and NUtE$_c$ has units of g dry wt. g^{-1} N. When NUtE is greater than NUtE$_c$, crop N

735 status is deficient (i.e., NNI less than 1); conversely, when NUtE is less than NUtE$_c$, crop N status

736 is excessive (i.e., NNI greater than 1).

737 The finding in the present study that the CNDC can vary across G × E × M interactions and the

738 finding from Bohman et al. (2021) of the intrinsic relationship between NUE and the CNDC

739 together lead to the conclusion that the CNUtEC must also vary across the same G × E × M effects

740 as the CNDC. Therefore, the effect of G × E x M on variation of NUtE$_c$ is one of the multiple set

741 of factors that ultimately control NUE. Understanding and accounting for the G × E × M effect on

742 the CNUtEC is therefore critically important to understand the impacts of G × E × M interactions

743 on NUE. In other words, controlling for this $G \times E \times M$ effect represents an additional requirement

744 when evaluating and interpreting NUE above and beyond the previously known requirements of

745 controlling for both NNI and biomass (Barraclough et al., 2010; Caviglia et al., 2014; Sadras &

746 Lemaire, 2014; Gastal et al., 2015; Lemaire & Ciampitti, 2020).

747 Following from the above discussion of the CNUtEC and the findings of Giletto et al. (2020), $G \times$

748 $E \times M$ effects that increase the relative proportion of biomass partitioned to tubers and reduce the

749 time to tuber initiation will both decrease the $\%N_c$ and increase the $NUtE_c$ values. Therefore, future

750 efforts to systematically improve NUE in potato through either management practices (e.g.,

751 Bohman et al. (2021)) or crop breeding (e.g., Tiwari et al. (2018); Jones et al. (2021); Stefaniak et

752 al. (2021)) should focus on identifying $G \times E \times M$ interactions that result in an increased proportion

753 of biomass partitioned to tubers or result in earlier timing of tuber initiation.

754 *4.3. Uncertainty in Critical N Concentration*

755 4.3.1. Communicating Uncertainty in Critical N Concentration

756 This study as well as others that implemented Bayesian statistical methods to derive critical N

757 dilution curves (Makowski et al., 2020; Ciampitti et al., 2021; Yao et al., 2021) clearly indicate

758 that there is meaningful uncertainty in $\%N_c$ values. Therefore, the use of $\%N_c$ in subsequent

759 calculations should include this inherent uncertainty. However, the direct use of the credible region

760 defined from posterior distribution of the fitted Bayesian hierarchical model in subsequent

761 calculations is impractical, and a method to concisely and accurately communicate the credible

762 region remains necessary.

763 Our finding that the credible region can be satisfactorily estimated using an equation of the same

764 form as the CNDC (Figure 6) suggests that an additional pair of negative exponential curves

765 representing the upper and lower boundary of the credible region for $\%N_c$ (i.e., $CNDC_{lo}$ and

766 $CNDC_{up}$) should be reported in future studies. In this manner, the median value and credible region

767 for $\%N_c$ is defined by a set of three, two-parameter curves (i.e., CNDC – a, b; $CNDC_{up}$ – a_{up}, b_{up};

768 $CNDC_{lo}$ – a_{lo}, b_{lo}) which can be easily communicated and used in subsequent computations (Table

769 7).

4.3.2. Computing Uncertainty of Derived Parameters

771 Critical N concentration and the associated CNDC parameters are commonly used to derive and

772 calculate other related parameters. For example, the calculation of NNI depends on both $\%N_{Plant}$

773 and $\%N_c$. (Eq. [1] and Eq. [2]). However, to properly account for the uncertainty in $\%N_c$ when

774 computing NNI, the upper [$\%N_{c,up}$] and lower [$\%N_{c,lo}$] bounds of the credible interval for $\%N_c$

775 should also be used to determine the upper [NNI_{up}] and lower [NNI_{lo}] bounds of the credible

776 interval for NNI, where $\%N_{c,up}$ and $\%N_{c,lo}$ are calculated using the $CNDC_{up}$ and $CNDC_{lo}$,

777 respectively:

778 $NNI_{up} = \%N_{Plant} \, / \, \%N_{c,up} = \%N_{Plant} \, / \, (a_{up} \, W^{-b}_{up})$ [9]

779 $NNI_{lo} = \%N_{Plant} \, / \, \%N_{c,lo} = \%N_{Plant} \, / \, (a_{lo} \, W^{-b}_{lo})$ [10]

780 This has important practical implications for interpreting NNI values. For example, in a case where

781 NNI is less than 1 but NNI_{up} is greater than 1, it follows that crop N status would not be considered

782 deficient (i.e., NNI is not significantly different from 1). In contrast, when both NNI and NNI_{lo} are

783 greater than 1, it follows that crop N status would be considered surplus (i.e., NNI is significantly

784 greater than 1). However, the threshold for considering significant differences in NNI will

785 necessarily depend upon the threshold used for calculating $\%N_{c,lo}$ and $\%N_{c,up}$ (e.g., 90%

786 confidence region). For example, the conclusions of a small-plot trial evaluating the effect of

787 various N fertilizer treatments on yield and biomass (e.g., Bohman et al. (2021)) may draw

788 different conclusions when uncertainty in calculated NNI values is explicitly considered (e.g., N

789 treatments were or were not limiting).

790 Additionally, the parameters of the CNDC (i.e., *a*, *b*) are also used to parameterize other related

791 curves such as the critical N uptake curve [CNUC] or the critical N utilization efficiency curve

792 [CNUtEC] (Bohman et al., 2021). When computing the critical N uptake [N_c] or critical N

793 utilization efficiency [$NUtE_c$] values defined by these curves, respectively, the parameters from

794 the $CNDC_{lo}$ (i.e., a_{lo}, b_{lo}) and $CNDC_{up}$ (i.e., a_{up}, b_{up}) should be used to calculate the upper and

795 lower bounds of these derived values. In general, any calculation depending on either $\%N_c$ or any

796 equation that uses the parameters of the CNDC, should also additionally use the $CNDC_{lo}$ and

797 $CNDC_{up}$ to account for uncertainty in $\%N_c$.

798 *4.4. Evaluating Differences between Statistical Methods*

799 While the occurrence of differences between CNDCs derived using the Bayesian hierarchical

800 model compared to the conventional statistical methods (Figure 7) is itself notable, the magnitude

801 of the differences found in the present study is especially remarkable for the following reasons.

802 Because of its strong theoretical underpinning, $\%N_c$ and NNI are typically considered to be high

803 fidelity measurements of crop N status, not affected by the subjectivity or relativity found in most

804 other methods (Lemaire et al., 2019). However, the findings of the present study strongly suggest

805 that this conception of the NNI framework must be qualified within a particular application by the

806 statistical methods used to derive the CNDC for a given experimental dataset.

807 Unfortunately, the direct evaluation of different statistical methods to calculate the CNDC from

808 the same experimental dataset cannot directly answer the question of which statistical method or

809 resulting CNDC is "correct" (i.e., most accurate, least biased). However, we can reasonably

810 conclude from both deduction and from the findings of the present study that a Bayesian

811 hierarchical model utilizing the linear-plateau method and leveraging partial pooling across effect

812 levels will result in inference that is less subjected to potential bias in the experimental data set

813 compared to the conventional statistical methods. Additionally, it extracts the greatest amount of

814 information from a given dataset, as no data are excluded from the fitting of the total model.

815 Therefore, it appears preferable for the future development of CNDCs to utilize the Bayesian

816 hierarchical method to both quantify uncertainty and reduce bias in $\%N_c$. Without addressing these

817 limitations (i.e., bias and uncertainty), both directly resulting from the statistical methods used, the

818 NNI framework cannot fulfill its core objective of providing an absolute reference of crop N status.

819 Additionally, with further development of standardized tools for this scientific computing task, the

820 implementation of the partially-pooled Bayesian hierarchical framework for deriving the CNDC

821 can be made trivial and may enable the development of CNDCs from existing but unutilized

822 experimental datasets. Therefore, the development of a dedicated software library to implement

823 the partially-pooled Bayesian hierarchical method developed in the present study is a priority for

824 future research efforts because it will enable other researchers to implement this preferred method

825 of deriving CNDCs.

826　Finally, having sufficient quantity and quality of experimental data remains an essential criteria to

827　consider when deriving a CNDC independent of the statistical method used (Fernández et al.,

828　2021; Fernández et al., 2022). Even with the advantages of the partially-pooled Bayesian

829　hierarchical method, insufficient experimental data quality and quantity may still result in

830　inferential bias of the CNDC for an individual $G \times E \times M$ interaction level. Given the limitations

831　of the quantity and quality of experimental data used in this study (i.e., bias towards N limiting

832　conditions for Argentina, bias towards non-N limiting conditions for Belgium and Minnesota), it

833　is plausible that estimates of CNDCs from this study are biased relative to estimates of CNDCs

834　derived using an "ideal" experimental dataset and identical statistical methods. Therefore, future

835　studies utilizing the partially-pooled Bayesian hierarchical method should ensure that the

836　experimental dataset for each $G \times E \times M$ interaction level meets the sufficiency criteria identified

837　by Fernández et al. (2022) (i.e., at least eight experimental trials containing at least three N

838　treatments and at least three sampling dates).

5. Conclusions

840　First, this study demonstrated that there are significant differences between CNDCs developed

841　across $G \times E \times M$ effects for potato. Therefore, any application of $\%N_c$ must use an appropriate

842　CNDC (i.e., not significantly different) for the $G \times E \times M$ interaction being considered. Second,

843　this study developed an approach to communicate uncertainty in $\%N_c$ through the concise set of

844　six parameters defined by the CNDC (i.e., a, b), $CNDC_{lo}$ (i.e., a_{lo}, b_{lo}), and $CNDC_{up}$ (i.e., a_{up}, b_{up}),

845　and the $\%N_c$ value computed from these three curves should be used in all subsequent

846　computations to propagate uncertainty. Third, this study demonstrated that the statistical method

847　used to derive CNDCs affects the inferred $\%N_c$ values, and that the partially-pooled hierarchical

848 Bayesian framework is less susceptible to bias due to insufficient quantity and quality of

849 experimental data than the conventional statistical methods. Therefore, future efforts to derive

850 CNDCs should utilize the partially-pooled hierarchical Bayesian framework whenever possible.

851 Fourth, the findings of this study suggest that variation in $\%N_c$ across $G \times E \times M$ interactions

852 necessarily extends to NUE, via the relationship between the CNDC and the CNUtEC. Therefore,

853 NUE is dependent on the mechanisms that control N dilution (i.e., biomass partitioning), and future

854 efforts to improve NUE should explicitly consider how $G \times E \times M$ interactions affect N dilution.

855

6. Acknowledgements

7. References

861 AHDB. (2015). Charlotte: Agriculture and Horticulture Development Board. Retrieved from
862 https://varieties.ahdb.org.uk/varieties/view/CHARLOTTE
863

864 Allen, E.J., and R.K. Scott. (1980). An Analysis of Growth of the Potato Crop. *J. Agr. Sci., 94*(3),
865 583-606. https://doi.org/10.1017/S0021859600028598.

866 Barraclough, P.B., J.R. Howarth, J. Jones, R. Lopez-Bellido, S. Parmar, C.E. Shepherd, and M.J.
867 Hawkesford. (2010). Nitrogen Efficiency of Wheat: Genotypic and Environmental
868 Variation and Prospects for Improvement. *Eur. J. Agron., 33*(1), 1-11.
869 https://doi.org/10.1016/j.eja.2010.01.005.

870 Bates, D.M. (2010). *Lme4: Mixed-Effects Modeling with R*.

871 Bélanger, G., J.R. Walsh, J.E. Richards, P.H. Milburn, and N. Ziadi. (2000). Yield Response of
872 Two Potato Culivars to Supplemental Irrigation and N Fertilization in New Brunswick.
873 *Am. J. Potato Res., 77*(1), 11-21. https://doi.org/10.1007/BF02853657.

874 Bélanger, G., J.R. Walsh, J.E. Richards, P.H. Milburn, and N. Ziadi. (2001a). Critical Nitrogen
875 Curve and Nitrogen Nutrition Index for Potato in Eastern Canada. *Am. J. Potato Res. ,*
876 *78*(5), 355-364. https://doi.org/10.1007/BF02884344.

877 Bélanger, G., J.R. Walsh, J.E. Richards, P.H. Milburn, and N. Ziadi. (2001b). Tuber Growth and
878 Biomass Partitioning of Two Potato Cultivars Grown under Different N Fertilization Rates
879 with and without Irrigation. *Am. J. Potato Res., 78*(2), 109-117.
880 https://doi.org/10.1007/BF02874766.

881 Ben Abdallah, F., M. Olivier, J.P. Goffart, and O. Minet. (2016). Establishing the Nitrogen
882 Dilution Curve for Potato Cultivar Bintje in Belgium. *Potato Res., 59*(3), 241-258.
883 https://doi.org/10.1007/s11540-016-9331-y.

884 Bennett, S.M., T.W. Tibbitts, and W. Cao. (1991). Diurnal Temperature Fluctuation Effects on
885 Potatoes Grown with 12 Hr Photoperiods. *Am. Potato. J., 68*, 81-86.
886 https://doi.org/10.1007/BF02853925.

887 Benoit, G.R., W.J. Grant, and O.J. Devine. (1986). Potato Top Growth as Influenced by Day-Night
888 Temperature Differences. *Agron. J., 78*(2), 264-269.
889 https://doi.org/10.2134/agronj1986.00021962007800020010x.

890 Bohman, B.J., M. McNearney, J. Crants, and C.J. Rosen. (2020). A Novel Approach to Manage
891 Nitrogen Fertilizer for Potato Production Using Remote Sensing. *Research Reports – 2020*.
892 Fargo, ND: Minnesota Area II Potato Research and Promotion Council and Northern Plains
893 Potato Growers Association. Retrieved from
894 https://www.ag.ndsu.edu/potatoextension/research/2020ResearchBooks.pdf

895 Bohman, B.J., C.J. Rosen, and D.J. Mulla. (2021). Relating Nitrogen Use Efficiency to Nitrogen
896 Nutrition Index for Evaluation of Agronomic and Environmental Outcomes in Potato.
897 *Field Crops Res., 262*. https://doi.org/10.1016/j.fcr.2020.108041.

898 Bremner, P.M., and M.A. Taha. (1966). Studies in Potato Agronomy. I. The Effects of Variety,
899 Seed Size and Spacing on Growth, Development and Yield. *The Journal of Agricultural*
900 *Science, 66*(2), 241-252. https://doi.org/10.1017/s0021859600062651.

901 Bürkner, P.-C. (2017). Brms: An R Package for Bayesian Multilevel Models Using Stan. *J. Stat.*
902 *Softw., 80*(1). https://doi.org/10.18637/jss.v080.i01.

903 Bürkner, P.-C. (2018). Advanced Bayesian Multilevel Modeling with the R Package Brms. *R J.,*
904 *10*(1), 395-411. https://doi.org/10.32614/RJ-2018-017.

905 Carpenter, B., A. Gelman, M.D. Hoffman, D. Lee, B. Goodrich, M. Betancourt, M. Brubaker, J.
906   Guo, P. Li, and A. Riddell. (2017). Stan: A Probabilistic Programming Language. *J. Stat.*
907   *Softw., 76*(1). https://doi.org/10.18637/jss.v076.i01.
908 Caviglia, O.P., R.J.M. Melchiori, and V.O. Sadras. (2014). Nitrogen Utilization Efficiency in
909   Maize as Affected by Hybrid and N Rate in Late-Sown Crops. *Field Crops Res., 168*, 27-
910   37. https://doi.org/10.1016/j.fcr.2014.08.005.
911 CFIA. (2013). Bintje: Canadian Food Inspection Agency. Retrieved from
912   https://inspection.canada.ca/plant-varieties/potatoes/potato-
913   varieties/bintje/eng/1312587385655/1312587385656
914 Ciampitti, I.A., J. Fernandez, S. Tamagno, B. Zhao, G. Lemaire, and D. Makowski. (2021). Does
915   the Critical N Dilution Curve for Maize Crop Vary across Genotype X Environment X
916   Management Scenarios? - a Bayesian Analysis. *Eur. J. Agron., 123*, 126202.
917   https://doi.org/10.1016/j.eja.2020.126202.
918 Crants, J., C. Rosen, M. McNearney, and L. Sun. (2017). The Use of Chlorophyll Meters for
919   Nitrogen Management in Potatoes. *Research Reports – 2017*. Fargo, ND: Minnesota Area
920   II Potato Research and Promotion Council and Northern Plains Potato Growers
921   Association. Retrieved from https://www.ag.ndsu.edu/potatoextension/research
922 Duchenne, T., J.M. Machet, and M. Martin. (1997). Potatoes. In G. Lemaire (Ed.), *Diagonsis of*
923   *the Nitrogen Status in Crops* (pp. 119-130). Berlin: Springer.
924 Egel, D.S. (2017). Midwest Vegetable Production Guide for Commercial Growers. *BU-07094-S*:
925   University of Minnesota Extension. Retrieved from https://ag.purdue.edu/btny/midwest-
926   vegetable-guide/Pages/default.aspx
927 Errebhi, M., C.J. Rosen, S.C. Gupta, and D.E. Birong. (1998). Potato Yield Response and Nitrate
928   Leaching as Influenced by Nitrogen Management. *Agron. J., 90*, 10-15.
929   https://doi.org/10.2134/agronj1998.00021962009000010003x.
930 Ewing, E.E., and P.C. Struik. (1992). Tuber Formation in Potato: Induction, Initiation, and Growth.
931   In J. Janick (Ed.), *Horticultural Reviews, Volume 14* (pp. 89-198): John Wiley & Sons.
932 Fernández, J.A., G. Lemaire, G. Bélanger, F. Gastal, D. Makowski, and I.A. Ciampitti. (2021).
933   Revisiting the Critical Nitrogen Dilution Curve for Tall Fescue: A Quantitative Synthesis.
934   *Eur. J. Agron., 131*, 126380. https://doi.org/10.1016/j.eja.2021.126380.
935 Fernandez, J.A., E. van Versendaal, J. Lacasa, D. Makowski, G. Lemaire, and I.A. Ciampitti.
936   (2022). Dataset Characteristics for the Determination of Critical Nitrogen Dilution Curves:
937   From Past to New Guidelines. *Eur. J. Agron., 139*, 126568.
938   https://doi.org/10.1016/j.eja.2022.126568.
939 Franzen, D., A. Robinson, and C. Rosen. (2018). Fertilizing Potato in North Dakota. *SF715*. Fargo,
940   ND: North Dakota State University. Retrieved from
941   https://www.ag.ndsu.edu/publications/crops/fertilizing-potato-in-north-dakota
942 Gastal, F., G. Lemaire, J.-L. Durand, and G. Louarn. (2015). Quantifying Crop Responses to
943   Nitrogen and Avenues to Improve Nitrogen-Use Efficiency. In *Crop Physiology* (Second
944   ed., pp. 161-206).
945 Gelaro, R., W. McCarty, M.J. Suarez, R. Todling, A. Molod, L. Takacs, C. Randles, A. Darmenov,
946   M.G. Bosilovich, R. Reichle, K. Wargan, L. Coy, R. Cullather, C. Draper, S. Akella, V.
947   Buchard, A. Conaty, A. da Silva, W. Gu, G.K. Kim, R. Koster, R. Lucchesi, D. Merkova,
948   J.E. Nielsen, G. Partyka, S. Pawson, W. Putman, M. Rienecker, S.D. Schubert, M.
949   Sienkiewicz, and B. Zhao. (2017). The Modern-Era Retrospective Analysis for Research

950 and Applications, Version 2 (Merra-2). *J Clim, Volume 30*(Iss 13), 5419-5454.
951 https://doi.org/10.1175/JCLI-D-16-0758.1.

952 Giletto, C.M., and H.E. Echeverría. (2015). Critical Nitrogen Dilution Curve in Processing Potato
953 Cultivars. *Am. J. Plant Sci., 06*(19), 3144-3156. https://doi.org/10.4236/ajps.2015.619306.

954 Giletto, C.M., N.I. Reussi Calvo, P. Sandaña, H.E. Echeverría, and G. Bélanger. (2020). Shoot-
955 and Tuber-Based Critical Nitrogen Dilution Curves for the Prediction of the N Status in
956 Potato. *Eur. J. Agron., 119*. https://doi.org/10.1016/j.eja.2020.126114.

957 Greenwood, D.J., G. Lemaire, G. Gosse, P. Cruz, A. Draycott, and J.J. Neeteson. (1990). Decline
958 in Percentage N of C3 and C4 Crops with Increasing Plant Mass. *Ann. Bot., 66*(4), 425-
959 436. https://doi.org/10.1093/oxfordjournals.aob.a088044.

960 Greenwood, D.J., J.J. Neeteson, and A. Draycott. (1986). Quantitative Relationships for the
961 Dependence of Growth Rate of Arable Crops on Their Nitrogen Content, Dry Weight and
962 Aerial Environment. *Plant Soil, 91*(3), 281-301. https://doi.org/10.1007/BF02198111.

963 Gupta, S., and C.J. Rosen. (2019). Nitrogen Fertilization Rate and Cold-Induced Sweetening in
964 Potato Tubers During Storage. *Research Reports – 2019*. Fargo, ND: Minnesota Area II
965 Potato Research and Promotion Council and Northern Plains Potato Growers Association.
966 Retrieved   from
967 https://www.ag.ndsu.edu/potatoextension/research/2019RESEARCHREPORTS.pdf

968 Gupta, S.K., J. Crants, M. McNearney, and C.J. Rosen. (2020). Evaluation of a Promising
969 Minnesota Clone for N Response, Agronomic Traits & Storage Quality. *Research Reports
970 – 2020*. Fargo, ND: Minnesota Area II Potato Research and Promotion Council and
971 Northern Plains Potato Growers Association. Retrieved from
972 https://www.ag.ndsu.edu/potatoextension/research/2020ResearchBooks.pdf

973 Hansen, B., and A.G. Giencke. (1988). Sand Plains Research Farm Soil Report. St. Paul, MN:
974 University of Minnesota

975 Herrmann, A., and F. Taube. (2004). The Range of the Critical Nitrogen Dilution Curve for Maize
976 (Zea Mays L.) Can Be Extended until Silage Maturity. *Agron. J., 96*(4), 1131-1138.
977 https://doi.org/10.2134/agronj2004.1131.

978 Horneck, D.A., and R.O. Miller. (1998). Determination of Total Nitrogen in Plant Tissue. In Y. P.
979 Kalra (Ed.), *Handbook of Reference Methods for Plant Analysis* (pp. 75-84). Boston: CRC
980 Press.

981 Horwitz, W., P. Chichilo, and H. Reynolds. (1970). *Official Methods of Analysis of the Association
982 of Official Analytical Chemists.* (11th ed.). Washington, DC: Association of Official
983 Analytical Chemists.

984 Houlès, V., M. Guérif, and B. Mary. (2007). Elaboration of a Nitrogen Nutrition Indicator for
985 Winter Wheat Based on Leaf Area Index and Chlorophyll Content for Making Nitrogen
986 Recommendations. *Eur. J. Agron., 27*(1), 1-11. https://doi.org/10.1016/j.eja.2006.10.001.

987 Ifenkwe, O.P., and E.J. Allen. (1978). Effects of Row Width and Planting Density on Growth and
988 Yield of Two Maincrop Potato Varieties. 1. Plant Morphology and Dry-Matter
989 Accumulation. *The Journal of Agricultural Science, 91*(2), 265-278.
990 https://doi.org/10.1017/s0021859600046359.

991 Jones, C.R., T.E. Michaels, C.S. Carley, C.J. Rosen, and L.M. Shannon. (2021). Nitrogen Uptake
992 and Utilization in Advanced Fresh-Market Red Potato Breeding Lines. *Crop Sci., 61*, 878–
993 895. https://doi.org/10.1002/csc2.20297.

994 Justes, E., B. Mary, J.-M. Meynard, J.-M. Machet, and L. Thelier-Huche. (1994). Determination
995   of a Critical Nitrogen Dilution Curve for Winter Wheat Crops. *Ann. Bot., 74*(4), 397-407.
996   https://doi.org/10.1006/anbo.1994.1133.

997 Kim, Y.U., and B.W. Lee. (2019). Differential Mechanisms of Potato Yield Loss Induced by High
998   Day and Night Temperatures During Tuber Initiation and Bulking: Photosynthesis and
999   Tuber Growth. *Front. Plant Sci., 10*, 300. https://doi.org/10.3389/fpls.2019.00300.

1000 Kleinkopf, G.E., D.T. Westermann, and R.B. Dwelle. (1981). Dry Matter Production and Nitrogen
1001   Utilization by Six Potato Cultivars. *Agron. J., 73*(5), 799-802.
1002   https://doi.org/10.2134/agronj1981.00021962007300050013x.

1003 Lemaire, G., and I. Ciampitti. (2020). Crop Mass and N Status as Prerequisite Covariables for
1004   Unraveling Nitrogen Use Efficiency across Genotype-by-Environment-by-Management
1005   Scenarios: A Review. *Plants, 9*(10). https://doi.org/10.3390/plants9101309.

1006 Lemaire, G., and F. Gastal. (1997). N Uptake and Distribution in Plant Canopies. In G. Lemaire
1007   (Ed.), *Diagnosis of the Nitrogen Status in Crops* (pp. 3-43). Berlin: Springer.

1008 Lemaire, G., T. Sinclair, V. Sadras, and G. Bélanger. (2019). Allometric Approach to Crop
1009   Nutrition and Implications for Crop Diagnosis and Phenotyping. A Review. *Agron.*
1010   *Sustain. Dev., 39*(2). https://doi.org/10.1007/s13593-019-0570-6.

1011 Li, D., Y. Miao, S.K. Gupta, C.J. Rosen, F. Yuan, C. Wang, L. Wang, and Y. Huang. (2021).
1012   Improving Potato Yield Prediction by Combining Cultivar Information and Uav Remote
1013   Sensing Data Using Machine Learning. *Remote Sens., 13*(16).
1014   https://doi.org/10.3390/rs13163322.

1015 Lindstrom, M.J., and D.M. Bates. (1990). Nonlinear Mixed Effects Models for Repeated Measures
1016   Data. *Biometrics, 46*(3), 673-687. https://doi.org/10.2307/2532087.

1017 Lizana, X.C., A. Avila, A. Tolaba, and J.P. Martinez. (2017). Field Responses of Potato to
1018   Increased Temperature During Tuber Bulking: Projection for Climate Change Scenarios,
1019   at High-Yield Environments of Southern Chile. *Agric. For. Meteorol., 239*, 192-201.
1020   https://doi.org/10.1016/j.agrformet.2017.03.012.

1021 Makowski, D., B. Zhao, S.T. Ata-Ul-Karim, and G. Lemaire. (2020). Analyzing Uncertainty in
1022   Critical Nitrogen Dilution Curves. *Eur. J. Agron., 118*.
1023   https://doi.org/10.1016/j.eja.2020.126076.

1024 McElreath, R. (2020). *Staistical Rethinking: A Bayesian Course with Examples in R and Stan* (2nd
1025   ed.). Boca Raton: Chapman and Hall/CRC.

1026 Menzel, C.M. (1985). Tuberization in Potato at High Temperatures: Interaction between
1027   Temperature and Irradiance. *Ann. Bot., 55*(1), 35-39.
1028   https://doi.org/10.1093/oxfordjournals.aob.a086875.

1029 Monteith, J.L. (1977). Climate and the Efficiency of Crop Production in Britain. *Phil. Trans. R.*
1030   *Soc. Lond. B, 281*, 277-294. https://doi.org/10.1098/rstb.1977.0140.

1031 Morier, T., A.N. Cambouris, and K. Chokmani. (2015). In-Season Nitrogen Status Assessment
1032   and Yield Estimation Using Hyperspectral Vegetation Indices in a Potato Crop. *Agron. J.,*
1033   *107*(4), 1295-1309. https://doi.org/10.2134/agronj14.0402.

1034 Morris, T.F., T.S. Murrell, D.B. Beegle, J.J. Camberato, R.B. Ferguson, J. Grove, Q. Ketterings,
1035   P.M. Kyveryga, C.A.M. Laboski, J.M. McGrath, J.J. Meisinger, J. Melkonian, B.N.
1036   Moebius-Clune, E.D. Nafziger, D. Osmond, J.E. Sawyer, P.C. Scharf, W. Smith, J.T.
1037   Spargo, H.M. van Es, and H. Yang. (2018). Strengths and Limitations of Nitrogen Rate
1038   Recommendations for Corn and Opportunities for Improvement. *Agron. J., 110*(1), 1.
1039   https://doi.org/10.2134/agronj2017.02.0112.

Nigon, T.J., C. Yang, D.J. Mulla, and D.E. Kaiser. (2019). Computing Uncertainty in the Optimum Nitrogen Rate Using a Generalized Cost Function. *Comput. Electron. Agric., 167*, 105030. https://doi.org/10.1016/j.compag.2019.105030.

OSU. (2021). Potato Variety Identification and Ownership Table: Oregon State University – Oregon Seed Certification Service. Retrieved from https://seedcert.oregonstate.edu/sites/seedcert.oregonstate.edu/files/potato_varietyratingk ey.pdf

Plénet, D., and G. Lemaire. (2000). Relationships between Dynamics of Nitrogen Uptake and Dry Matter Accumulation in Maize Crops. Determination of Critical N Concentration. *Plant Soil, 216*(1/2), 65-82. https://doi.org/10.1023/a:1004783431055.

Plummer, M. (2013). Jags: Just Another Gibs Sampler. Retrieved from http://mcmc-jags.sourceforge.net/.

Plummer, M. (2019). Rjags: Bayesian Graphical Models Using Mcmc. Retrieved from https://CRAN.R-project.org/package=rjags

Porter, G. (2014). 201400091. USDA PVPO.

R Core Team. (2021a). R: A Language and Environment for Statistical Computing. Vienna, Austria: R Foundation for Statistical Computing. Retrieved from https://www.R-project.org/

R Core Team. (2021b). "Stats": The R Stats Package. Retrieved from https://CRAN.R-project.org/package=stats

Rosen, C., D. Birong, and M. Zumwinkle. (1992). Nitrogen Fertilization Studies on Irrigated Potatoes: Nitrogen Use, Soil Nitrate Movement, and Petiole Sap Nitrate Analysis for Predicting Nitrogen Needs. *Field Research in Soil Science – Soil Series #134*. St. Paul, MN: University of Minnesota. Retrieved from https://conservancy.umn.edu/handle/11299/121705

Rosen, C., J. Crants, B. Bohman, and M. McNearney. (2021). Effects of Banded Versus Broadcast Application of Esn, Turkey Manure, and Different Approaches to Measuring Plant N Status on Tuber Yield and Quality in Russet Burbank Potatoes. *Reserach Reports – 2021*. Fargo, ND: Minnesota Area II Potato Research and Promotion Council and Northern Plains Potato Growers Association. Retrieved from https://www.ag.ndsu.edu/potatoextension/research/research_reports_114_4126022392.pd f

Rosen, C., M. Errebhi, J. Moncrief, S. Gupta, H.H. Cheng, and D. Birong. (1993). Nitrogen Fertilization Studies on Irrigated Potatoes: Nitrogen Use, Soil Nitrate Movement, and Petiole Sap Nitrate Analysis for Predicting Nitrogen Needs. *Field Research in Soil Science – Soil Series #136*. St. Paul, MN: University of Minnesota. Retrieved from https://conservancy.umn.edu/handle/11299/121706

Rosen, C.J. (2018). Potato Fertilization on Irrigated Soils: University of Minnesota Extension. Retrieved from https://extension.umn.edu/crop-specific-needs/potato-fertilization-irrigated-soils

Sadras, V.O., and G. Lemaire. (2014). Quantifying Crop Nitrogen Status for Comparisons of Agronomic Practices and Genotypes. *Field Crops Res., 164*, 54-64. https://doi.org/10.1016/j.fcr.2014.05.006.

Schad, D.J., M. Betancourt, and S. Vasishth. (2021). Toward a Principled Bayesian Workflow in Cognitive Science. *Psychol Methods, 26*(1), 103-126. https://doi.org/10.1037/met0000275.

Sinclair, T.R., and R.C. Muchow. (1999). Radiation Use Efficiency. In D. L. Sparks (Ed.), *Advances in Agronomy, Volume 65* (Vol. 65, pp. 215-265).

Slater, J.W. (1968). The Effect of Night Temperature on Tuber Initiation of the Potato. *European Potato Journal, 11*(1), 14-22. https://doi.org/10.1007/BF02365158.

Stark, J.C., A.L. Thompson, R. Novy, and S.L. Love. (2020). Variety Selection and Management. In J. C. Stark, M. Thornton, and P. Nolte (Eds.), *Potato Production Systems* (pp. 35-64).

Steele, D.D., T.F. Scherer, J. Wright, D.G. Hopkins, S.R. Tuscherer, and J. Wright. (2010). Spreadsheet Implementation of Irrigation Scheduling by the Checkbook Method for North Dakota and Minnesota. *Appl. Eng. Agric., 26*, 983-996. https://doi.org/10.13031/2013.35914.

Stefaniak, T.R., S. Fitzcollins, R. Figueroa, A.L. Thompson, C. Schmitz Carley, and L.M. Shannon. (2021). Genotype and Variable Nitrogen Effects on Tuber Yield and Quality for Red Fresh Market Potatoes in Minnesota. *Agronomy, 11*, 255. https://doi.org/10.3390/agronomy11020255.

Sun, N. (2017). *Agronomic and Storage Factors Affecting Acrylamide Formation in Processed Potatoes.* (Ph.D.). University of Minnesota, St. Paul, MN. Retrieved from https://conservancy.umn.edu/handle/11299/190488

Sun, N., Y. Wang, S.K. Gupta, and C.J. Rosen. (2019). Nitrogen Fertility and Cultivar Effects on Potato Agronomic Properties and Acrylamide-Forming Potential. *Agron. J., 111*(1), 408. https://doi.org/10.2134/agronj2018.05.0350.

Sun, N., Y. Wang, S.K. Gupta, and C.J. Rosen. (2020). Potato Tuber Chemical Properties in Storage as Affected by Cultivar and Nitrogen Rate: Implications for Acrylamide Formation. *Foods, 9*(3). https://doi.org/10.3390/foods9030352.

Thompson, A. (2013). 201300475. USDA PVPO.

Thornton, M. (2020). Potato Growth and Development. In J. C. Stark, M. Thornton, and P. Nolte (Eds.), *Potato Production Systems* (pp. 19-33).

Tiwari, J.K., D. Plett, T. Garnett, S.K. Chakrabarti, and R.K. Singh. (2018). Integrated Genomics, Physiology and Breeding Approaches for Improving Nitrogen Use Efficiency in Potato: Translating Knowledge from Other Crops. *Funct. Plant Biol., 45*(6), 587. https://doi.org/10.1071/fp17303.

USDA. (1997). United States Standards for Grades of Potatoes for Processing. Retrieved from https://www.ams.usda.gov/sites/default/files/media/Potatoes_for_Processing_Standard%5B1%5D.pdf

USDA NRCS. (2013). Soil Series Classification Database – Hubbard Series: United States Department of Agriculture. Retrieved from https://soilseries.sc.egov.usda.gov/OSD_Docs/H/HUBBARD.html

Ushey, K. (2021). Renv: Project Environments. Retrieved from https://CRAN.R-project.org/package=renv

Vander Zaag, P., A.L. Demagante, and E.E. Ewing. (1990). Influence of Plant Spacing on Potato (Solanum Tuberosum L.) Morphology, Growth and Yield under Two Contrasting Environments. *Potato Res., 33*(313–323). https://doi.org/10.1007/BF02359305.

Weather Spark. (2021). Compare the Climate and Weather in Becker, Saint-Léonard, Balcarce, and Gembloux. Retrieved from https://weatherspark.com/compare/y/10443~27617~28950~51092/Comparison-of-the-Average-Weather-in-Becker-Saint-L%C3%A9onard-Balcarce-and-Gembloux

1130   Wright, J. (2002). Irrigation Scheduling Checkbook Method. *BU-FO-01322*. St. Paul, MN:
1131   University of Minnesota. Retrieved from https://extension.umn.edu/irrigation/irrigation-
1132   scheduling-checkbook-method

1133   Yao, B., X. Wang, G. Lemaire, D. Makowski, Q. Cao, X. Liu, L. Liu, B. Liu, Y. Zhu, W. Cao, and
1134   L. Tang. (2021). Uncertainty Analysis of Critical Nitrogen Dilution Curves for Wheat. *Eur.*
1135   *J. Agron., 128*, 126315. https://doi.org/10.1016/j.eja.2021.126315.

1136

Click here to access/download
Supplementary material for on-line publication only
bayesian-cndc-potato_eja-submission_supplement-v1.docx

Click here to access/download
Supplementary material for on-line publication only
bayesian-cndc-potato_eja-submission_supplement-
v1.xlsx

Declaration of interests

☐The authors declare that they have no known competing financial interests or personal relationships that could have appeared to influence the work reported in this paper.

☒The authors declare the following financial interests/personal relationships which may be considered as potential competing interests:

Carl J. Rosen reports financial support was provided by Minnesota Area II Potato Growers Research and Promotion Council.